

Decays of doubly charmed meson molecules

R. Molina¹, H. Nagahiro² and A. Hosaka¹

October 16, 2018

¹ Research Center for Nuclear Physics (RCNP), Osaka University, Ibaraki, Osaka 567-0047, Japan

² Department of Physics, Nara Women's University, Nara 630-8506, Japan

Abstract

Several observed states close to the $D\bar{D}^*$ and $D_{(s)}^*\bar{D}_{(s)}^*$ thresholds, as the X(3872) and some XYZ particles can be described in terms of a two-meson molecule. Furthermore, doubly charmed states are also predicted. These new states are near the D^*D^* and $D^*D_s^*$ thresholds, and have spin-parity $J^P = 1^+$. Their natural decay modes are $D_{(s)}D^*$, $DD_{(s)}\pi$ and $DD_{(s)}\gamma$ and $D^*D_{(s)}\gamma$. We evaluate the widths of these states, named here as $R_{cc}(3970)$ and $S_{cc}(4100)$, and obtain 44 MeV for the non-strangeness, and 24 MeV for the doubly charm-strange state. Essentially, the decay modes are $DD_{(s)}\pi$ and $DD_{(s)}\gamma$, being the $D\pi$ and $D\gamma$ emitted by one of the D^* meson which forms the molecule.

1 Introduction

Since the discovery of the X(3872) by the Belle Collaboration [1], and observed afterwards by other collaborations, the number of so-called XYZ states have been increasing. The next by mass are X(3915), X(3940), Y(3940), Z(3930) and X(4160). Most of these states cannot be fitted in terms of $c\bar{c}$ [2]. For example, it is difficult to accommodate the X(3872) in the charmonium spectra because the ratio $\Gamma(X \rightarrow \pi^+\pi^-J/\psi)/\Gamma(X \rightarrow \pi^0\pi^+\pi^-)$ gives large branching fraction to $\pi^+\pi^-J/\psi$, which is unexpected for the available charmonium assignments, χ'_{c1} ($2^3P_1 c\bar{c}$) or 2^{-+} , η_{c2} . Instead, it is often said that the X(3872) could be a molecule made of $D\bar{D}^*$ [3, 4], which is strongly reinforced by the mass so-close to these thresholds. A clear explanation of this issue has been given in [5, 6], where, based on a molecular picture with an interaction provided by hidden gauge lagrangians [7, 8], the authors found that it is possible to explain the ratio $\Gamma(X \rightarrow \pi^+\pi^-J/\psi)/\Gamma(X \rightarrow \pi^0\pi^+\pi^-J/\psi)$ as a molecular object of $I = 0$ with a mixture of a very small component of $I = 1$. Moreover, to explain the missing charged partner and $\chi_{c1}(2P)$, and some reaction rates such as the production from the $p\bar{p}$ collision, a hybrid picture with a $\bar{c}c$ -core was also proposed [9]. While a small fraction of the quark core is needed for the above features, it

was shown that the main component of the $X(3872)$ is the $D\bar{D}^*$ molecule. Recently, the LHCb has measured [10] the quantum numbers of the $X(3872)$ as 1^{++} . This result rules out the $X(3872)$ to be the $\eta_{c2}(1^1D_2)$ state, favoring the exotic interpretation.

It has been discussed by several authors whether or not some of the other observed XYZ particles can be described in terms of molecules [11–20]. Regarding the observed states near to the $D^*\bar{D}^*$ thresholds, using the same formalism as in [5] for the $X(3872)$, with hidden gauge Lagrangians, some of the XYZ states [2] can also be interpreted as $D_{(s)}^*\bar{D}_{(s)}^*$ -like molecules [11]. In [11], three states with $I = 0$ and $J^{PC} = 0^{++}, 1^{+-}$ and 2^{++} around 3940 MeV are found, other with $I[J^{PC}] = 0[2^{++}]$ and mass close to 4160 MeV, and also a Z_c charged state with mass around 3920 MeV and quantum numbers $I[J^{PC}] = 1[2^{++}]$ (see next section for further discussion). Furthermore, in [21] the authors show that the dynamics from the extrapolation of the local hidden gauge model to $SU(4)$ fully respects the constraints of heavy quark spin symmetry. In [12], the authors start from the assumption that the $Y(3940)$ and the $Y(4140)$ are hadronic molecules with quantum numbers $J^{PC} = 0^{++}$ or 2^{++} whose constituents are the charm vectors $D^*\bar{D}^*$ for the $Y(3940)$ and $D_s^{*+}\bar{D}_s^{*-}$ for the $Y(4140)$ and they calculate the decay rates of the observed modes $Y(3940) \rightarrow J/\psi\omega$ and $Y(4140) \rightarrow J/\psi\phi$ for the case $J^{PC} = 0^{++}$. Their results for the coupling constants are the input to evaluate the decay modes that supports the molecular interpretation. In [13], the authors present an EFT (Effective Field Theory) description of heavy mesons molecules based on HQSS (Heavy Quark Spin Symmetry), and predict in total six $D^{(*)}\bar{D}^{(*)}$ molecular states based on the assumption that the $X(3915)$ is a 0^{++} heavy spin symmetry partner of the $X(3872)$.

The molecular picture can also be applied to further states, though the vector-vector interaction does not always provide sufficient attraction. Only those carrying the quantum number *hidden charm* ($C = 0; S = 0$), ($C = 1; S = -1, 0, 1$) and ($C = 2; S = 0, 1$), form molecules of two D^* mesons or D^* and ρ, K^* [22, 23]. Some of these cases are flavour exotics since they can not be reached by $q\bar{q}$ [23]. Of particular interest is the doubly charmed states of $C = 2$, which is a challenge also for experiments. Doubly charm states with the same quantum numbers have also been found in [24] from solving the scattering problem of two D -mesons with the interaction provided by the chiral constituent quark model. Theoretically, tetraquark structure has been also discussed [25–27]. In [25], the authors assume that the $X(3872)$ is a tetraquark structure and use its mass as input to determine the mass of the T_{cc} , finding $M_{T_{cc}} = 3966$ MeV. Whether they exist or not, and if so what their structure would be like, either molecular or compact tetraquark like, is an important question.

On the whole, using the hidden gauge Lagrangians together with unitary scattering amplitudes, it is possible to obtain, the doubly charmed $R_{cc}^+(3970)$ and $S_{cc}^{+(+)}(4100)$ as dynamically generated states from the vector-vector interaction with the same value of the free parameters (the subtraction constant or cutoff in the two-meson function loop) to those used for the XYZ [11] (this is shown in the next section). Therefore, if some of these states, like the $Y(3940)$ or $X(4160)$, are good candidates of meson-molecular states, we strongly expect that there also should be doubly charmed mesons.

To explore further the internal structure of these states, it is useful to study various transition amplitudes, including production and decays. In this paper, we study the decays of the predicted exotic states of $D^*D_{(s)}^*$ molecules in detail. The production mechanism perhaps requires combinations of hard and soft processes which is beyond our scope in the present paper. Because of a bosonic system, a D^*D^* molecule can form a state of spin and parity $J^P = 1^+$ when they are dominated by an s-wave state. They cannot decay into $D\bar{D}$ due to its quantum numbers. In this paper we consider possible decays of $R_{cc}(3970)$ and $S_{cc}(4100)$, including strong and radiative decays. The strong decays occur through $DD_{(s)}^*$ or $D_{(s)}D^*$ which subsequently go to three body states via $D^* \rightarrow \pi D$. Radiative decays also occur through the above two-body channels with $D^* \rightarrow D\gamma$. There are also direct decays into three-body states, $DD\gamma$, but they are small as compared to the above processes going through two bodies, as we show in this manuscript.

The structure of the paper is as follows. First, we explain briefly the model for the dynamically generated resonances, XYZ and doubly charm states, in section 2. In section 3, we evaluate their decay widths to $D_{(s)}D_{(s)}^*$, which are mediated by vector mesons or pseudoscalar ones. Direct three-body radiative decays are studied in section 4 and 5. Finally, in sections 6 we show the results reaching the conclusions and final remarks in section 7.

2 Dynamically generated XYZ, doubly charm mesons and the breaking of the $SU(4)$ symmetry

In our approach, local hidden gauge lagrangians are used to study the vector-vector interaction [11, 22, 23, 28, 29]. The hidden gauge Lagrangian, which involves the interaction of vector mesons amongst themselves, coming from the formalism of the hidden gauge symmetry (HGS) for vector mesons [7, 8]

$$\mathcal{L}_{III} = -\frac{1}{4}\langle V_{\mu\nu}V^{\mu\nu} \rangle, \quad (1)$$

where the symbol $\langle \rangle$ stands for the trace in the $SU(4)$ space and $V_{\mu\nu}$ is given by

$$V_{\mu\nu} = \partial_\mu V_\nu - \partial_\nu V_\mu - ig[V_\mu, V_\nu], \quad (2)$$

with g given by

$$g = \frac{M_V}{2f}, \quad (3)$$

and $f = 93$ MeV the pion decay constant. Using the value of g in Eq. (3) is one of the ways to account for the KSFR relation [30] which is tied to vector meson dominance [31]. The vector field V_μ is represented by the $SU(4)$ matrix which is parametrized by 16 vector

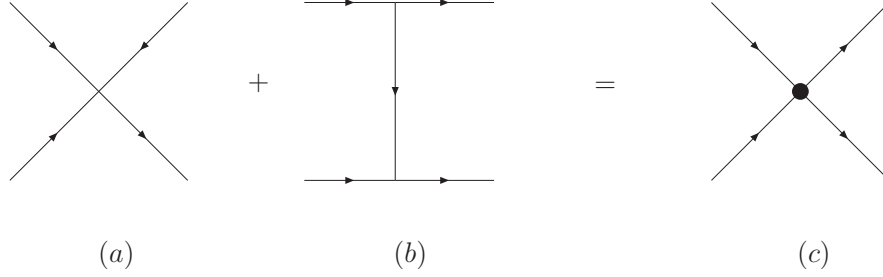


Figure 1: Feynman diagrams for the vector - vector interaction, contact term (a) and vector exchange (b) are included in the kernel V [23].

mesons including the 15-plet and singlet of $SU(4)$,

$$V_\mu = \begin{pmatrix} \frac{\rho^0}{\sqrt{2}} + \frac{\omega}{\sqrt{2}} & \rho^+ & K^{*+} & \bar{D}^{*0} \\ \rho^- & -\frac{\rho^0}{\sqrt{2}} + \frac{\omega}{\sqrt{2}} & K^{*0} & D^{*-} \\ K^{*-} & \bar{K}^{*0} & \phi & D_s^{*-} \\ D^{*0} & D^{*+} & D_s^{*+} & J/\psi \end{pmatrix}_\mu, \quad (4)$$

where the ideal mixing has been taken for ω , ϕ and J/ψ . The interaction of \mathcal{L}_{III} gives rise to a contact term

$$\mathcal{L}_{III}^{(c)} = \frac{g^2}{2} \langle V_\mu V_\nu V^\mu V^\nu - V_\nu V_\mu V^\mu V^\nu \rangle, \quad (5)$$

depicted in Fig. 1 (a), and also to a three vector vertex [28, 29]

$$\mathcal{L}_{3V} = ig \langle (V^\mu \partial_\nu V_\mu - \partial_\nu V_\mu V^\mu) V^\nu \rangle. \quad (6)$$

This latter Lagrangian gives rise to a $VV \rightarrow VV$ amplitude by means of the exchange of one of the vectors, as shown in Figs. 1 (b). The vector-exchange diagram in Fig. 1 (b) dominates the interaction (in the sectors $charm = 2$; $strangeness = 0, 1$, only the potential from this diagram survives) and upon the approximation $q^2 \sim 0$ leads to a contact interaction, see Fig. 2. In some channels it is attractive and leads to the generation of bound states in the coupled channel calculation [11]. The potential from Fig. 1 (b) after spin projection can be read as:

$$V_{ij} = - \frac{g^2}{m_{V_{ex}}^2} A_{ij}(s-u) \quad \text{for } J = 0, 1, 2, \quad (7)$$

in the t -channel and

$$\begin{aligned} V_{ij} &= - \frac{g^2}{m_{V_{ex}}^2} B_{ij}(s-t) \quad \text{for } J = 0, 2, \\ V_{ij} &= \frac{g^2}{m_{V_{ex}}^2} B_{ij}(s-t) \quad \text{for } J = 1, \end{aligned} \quad (8)$$

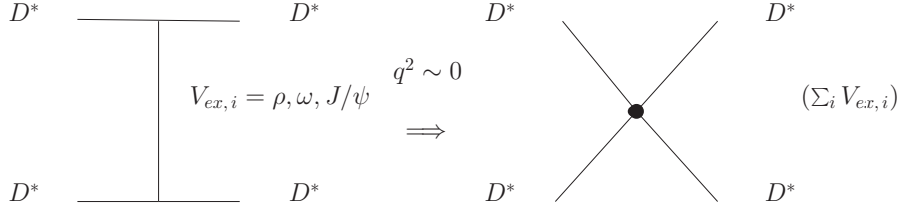


Figure 2: Point-like vector-vector interaction in the case of $D^*D^* \rightarrow D^*D^*$.

in the u -channel. Here, $m_{V_{ex}}$ stands for the mass of the exchanged vector meson, A_{ij}, B_{ij} are the coefficients for the particular transitions $i \rightarrow j$, and $g = m_V/(2f)$.

The $SU(4)$ structure of the Lagrangian allows us to take into account all possible particle channels by a single interaction term. However, in reality, the $SU(4)$ flavour symmetry is broken in several ways:

- 1) All the physical masses are taken from the PDG [32]. The strength of the s -wave projected potential of Eq. (8) increases with the initial energy s , which leads to a stronger potential when D^* particles are involved than for lighter vector mesons.
- 2) The exchange of heavy particles like J/ψ is suppressed compared to ρ, ω or ϕ due to the presence of $m_{V_{ex}}^2$ in the denominator.
- 3) Different coupling constants “ g ” in Eqs. (5), (6) and (8) are taken, “ g_h^2 ” for $V_h V_h \rightarrow V_h V_h$, “ $g_h g_l$ ” for $V_h V_h \rightarrow V_l V_l$, and “ g_l^2 ” for $V_l V_l \rightarrow V_l V_l$, where h means heavy particle, $h = D^*, D_s^*$ and l light particle. Thus different coupling constants are used $g_{D^*} = m_{D^*}/(2f_D)$, $g_{D_s^*}$ or $g = m_\rho/(2f_\pi)$, with $f_D = 206/\sqrt{2}$ MeV and $f_\pi = 93$ MeV in [11].

The sum of the amplitudes in Fig. 1, projected in s -wave, isospin and spin, are the kernel of the Bethe Salpeter equation used to unitarize amplitudes resumming over loops [33].

$$T = (\hat{1} - VG)^{-1}V . \quad (9)$$

The potential V here is a 10×10 matrix in $I = 0$ with the amplitudes obtained from the channels $D^* \bar{D}^*$, $D_s^* \bar{D}_s^*$, $K^* \bar{K}^*$, $\rho\rho$, $\omega\omega$, $\phi\phi$, $J/\psi J/\psi$, $\omega J/\psi$, $\phi J/\psi$, $\omega\phi$, in its elements for each spin $J = 0, 1, 2$ independently. Also, in $I = 1$, V is a 6×6 matrix whose elements come from the transition potentials between the channels $D^* \bar{D}^*$, $K^* \bar{K}^*$, $\rho\rho$, $\rho\omega$, $\rho J\psi$, $\rho\phi$, and G is a diagonal matrix where its elements are the two meson loop function $G_i(P)$ for each channel i

$$G_i(P) = i \int \frac{d^4 q}{(2\pi)^4} \frac{1}{q^2 - m_1^2 + i\epsilon} \frac{1}{(P - q)^2 - m_2^2 + i\epsilon} , \quad (10)$$

where P is the initial four-momentum, with $P^0 = \sqrt{s}$. $G_i(P)$ is a function of $\alpha(\mu)$ in the dimensional regularization scheme, or q_{\max} if the cutoff method is used instead. The result

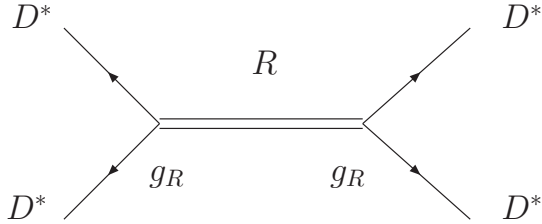


Figure 3: Couplings of the resonance to the two vector meson component.

of the calculation gives the poles positions in the complex plain and the coupling constant of the state, g_R , to the two meson component in each channel, evaluated as the square root of the residue of the pole in this channel, see Fig. 3. This coupling constant g_R and the pole positions, $\sqrt{s_0}$, are the only magnitudes needed to evaluate observables as decay widths.

To investigate the effect of the SU(4) breaking, we have performed the calculation of [11] by using two parameter sets: 1) with SU(4) symmetric coupling, $g_l = m_\rho/(2f_\pi)$ in Eqs. (5), (6) and $\alpha_h = -1.4$ ($\mu = 1500$ MeV) in all channels, and 2) with SU(4) breaking couplings, we use g_h^2 or $g_l g_h$, being $g_h = m_{D^*}/(2f_D)$ in the channels involving heavy particles as explained before in this section, and $\alpha_h = -1.27$. The results are shown in the Tables 4 and 5 in the Appendix (A.1), where pole positions, $\sqrt{s_0}$, and couplings to the two-meson channel of the resonance, g_R are summarized. From these tables, we can see that: 1) the use of different g_l or g_h in the heavy channels is mostly compensated by a small change of α_h . 2) the value of the coupling of the resonance, g_R , to the most important channel, $D^* \bar{D}^*$ or $D_s^* \bar{D}_s^*$, barely changes using one or the other prescription. The conclusion is that the different value of the coupling g in SU(3), for heavy particles, can be absorbed into the change in the subtraction constant α_h .

In this article we refer to those states obtained in [23] in the sectors $charm = 2$; $strangeness = 0, 1$, where only one channel is possible, $D^* D^*$ or $D^* D_s^*$, as $R_{cc}(3970)$ and $S_{cc}(4100)$. These bound states have quantum numbers $I[J^P] = 0[1^+]$ and $I[J^P] = 1/2[1^+]$, respectively.

The amplitude in Fig. 3 shows diagrammatically the coupling of the R_{cc} (S_{cc}) resonance to $D^* D^*$, $D^* D_s^*$. For the couplings of the resonance to the two vectors, keeping the $spin = 1$ structure, the resulting T -matrix amplitude $T(D^* D^* \rightarrow D^* D^*)$ can be approximated in the vicinity of the pole as

$$T \simeq \frac{[g_R \frac{1}{2}(\epsilon_1^i \epsilon_2^j - \epsilon_1^j \epsilon_2^i)][g_R \frac{1}{2}(\epsilon_1^i \epsilon_2^j - \epsilon_2^j \epsilon_1^i)]}{s - s_p} \quad (11)$$

Using the two sets of parameters, 1) g_l with $\alpha_h = -1.4$, or 2) g_h with $\alpha_h = -1.27$, to obtain the $I = 0$ states around 3940 MeV as described above, we evaluate the pole positions and couplings of the resonance for the doubly charm states. The results are summarized in Table 1. In this table we show the value of the coupling to the most

important channel comparing both assumptions. As we observe under these two different situations, the changes in the masses and coupling constants are small, in particular the resulting coupling constants are similar to those obtained by the Weinberg's formula,

$$\frac{g_W^2}{4\pi} = 4(m_1 + m_2)^2 \sqrt{\frac{2B}{\mu}} \left[1 + O\left(\frac{\sqrt{2\mu B}}{\beta}\right)\right] \quad (12)$$

where $m_{1,2}$ are the constituent masses, B is the binding energy of the molecule with mass M , defined as $M = m_1 + m_2 - B$, μ is the reduced mass and $1/\beta$ the range of the forces [34, 35]. We obtain in both cases doubly charm states. Their couplings to $D^*D_{(s)}^*$ are used to evaluate their decay widths in the next section.

From Table 1, we see, for only one channel as the case of doubly charm mesons (D^*D^* or $D^*D_s^*$), the decrease in the mass reverts into a larger couplings, which is consistent with the formula of Weinberg.

This effect of bigger coupling for lower masses will be taken into account in this paper when we perform the calculation of the errors of the decay widths.

$C; S$	I, J	M_R		channel	$ g_R $		g_{eff}^W	
		(g_l)	(g_h)		(g_l)	(g_h)	(g_l)	(g_h)
0; 0	0, 0	3936	3950	$D^*\bar{D}^*$	18700	18000	18050	17200
	0, 1	3940	3955	$D^*\bar{D}^*$	18260	17200	17800	16900
	0, 2	3921	3922	$D^*\bar{D}^*$	20600	21000	18800	18800
	0, 2	4174	4160	$D_s^*\bar{D}_s^*$	20400	19500	16700	17700
	1, 2	3970	3924	$D^*\bar{D}^*$	20500	20560	15800	18700
2; 0	0, 1	3968	3942	D^*D^*	16800	19500	15900	17800
2; 1	1/2, 1	4100	4070	$D_s^*D^*$	13400	17700	13100	16400

Table 1: Mass of the dynamically generated XYZ, doubly charm resonances, and the coupling to the main channel using g_l and $\alpha_h = -1.4$ or g_h , with $\alpha_h = -1.27$ in the channels with heavy vector mesons. Units are MeV.

3 Decays of doubly charmed states to $D_{(s)}D_{(s)}^*$

The $R_{cc} \rightarrow DD_{(s)}^*$ transition can be reached through anomalous couplings VVP (where the symbol R_{cc} stands for the doubly charmed resonance). The set of Feynman diagrams considered are depicted in Fig. 4. Within loops, particles cannot be distinguished and we must consider different sign of the isospin factor in the isospin combination:

$$|D^*D^*, I = 0, I_3 = 0\rangle = \frac{1}{\sqrt{2}}(-D^{*+}D^{*0} + D^{*0}D^{*+}) \quad (13)$$

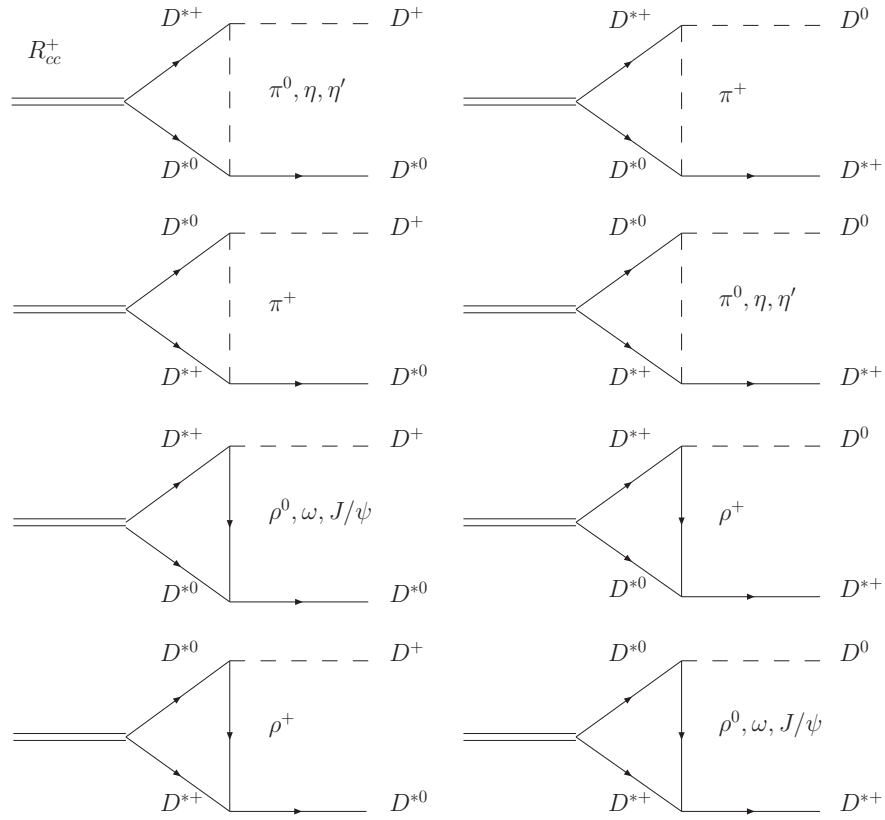


Figure 4: Feynman diagrams evaluated in the decay $R_{cc}^+ \rightarrow DD^*$.

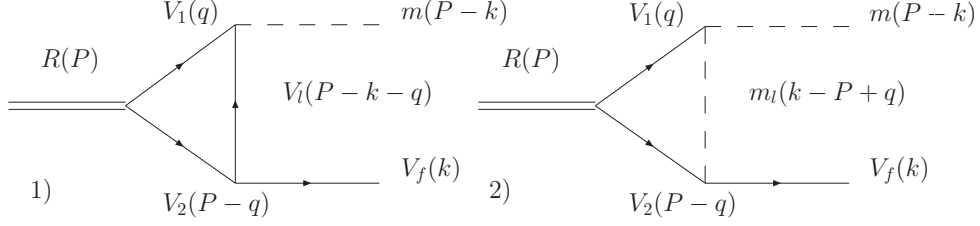


Figure 5: PPV and 3V Feynman diagrams for the evaluation of the $R_{cc} \rightarrow DD^*_{(s)}$ decay width.

with $D^{*+} = |\frac{1}{2}, \frac{1}{2}\rangle$ and $D^{*0} = -|\frac{1}{2}, -\frac{1}{2}\rangle$. While for the strange doubly charmed state, we have $|D^*D^*_s, I = \frac{1}{2}, I_3 = -\frac{1}{2}\rangle = -D^{*0}D^{*+}_s$ and $|D^*D^*_s, I = \frac{1}{2}, I_3 = \frac{1}{2}\rangle = D^{*+}D^{*+}_s$. The couplings of the resonances to the D^*D^* component are given in Table 1 in the isospin basis, using two different prescriptions: 1) $\alpha_h = -1.4$ and $g_l = m_\rho/(2f_\pi)$, 2) $\alpha_h = -1.27$ and $g_h = m_{D^*}/(2f_D)$. We will use the first prescription and perform variations of the parameters involved afterwards (see section 6).

The Lagrangians needed to evaluate the decay width to $DD^*_{(s)}$ are [8],

$$\begin{aligned}
\mathcal{L}_{PPV} &= -ig\langle V^\mu [P, \partial_\mu P] \rangle \\
\mathcal{L}_{3V} &= ig\langle (V^\mu \partial_\nu V_\mu - \partial_\nu V_\mu V^\mu) V^\nu \rangle \\
\mathcal{L}_{VVP} &= \frac{G'}{\sqrt{2}} \epsilon^{\mu\nu\alpha\beta} \langle \partial_\mu V_\nu \partial_\alpha V_\beta P \rangle,
\end{aligned} \tag{14}$$

with e the unit electronic charge ($e^2/4\pi = \alpha$), $G' = 3g'^2/(4\pi^2 f)$, $g' = -G_V M_\rho/(\sqrt{2}f^2)$, $G_V = f/\sqrt{2}$ and $g = M_V/2f$. The constant f is the pion decay constant $f = 93 \text{ MeV}$, $Q = \text{diag}(2, -1, -1, 1)/3$ and M_V is the mass of the vector meson.

The P matrix contain the 15-plet of the pseudoscalars and the 15-plet of vectors respectively in the physical basis considering η, η' mixing [36]:

$$P = \begin{pmatrix} \frac{\eta}{\sqrt{3}} + \frac{\eta'}{\sqrt{6}} + \frac{\pi^0}{\sqrt{2}} & \pi^+ & K^+ & \bar{D}^0 \\ \pi^- & \frac{\eta}{\sqrt{3}} + \frac{\eta'}{\sqrt{6}} - \frac{\pi^0}{\sqrt{2}} & K^0 & D^- \\ K^- & \bar{K}^0 & -\frac{\eta}{\sqrt{3}} + \sqrt{\frac{2}{3}}\eta' & D^-_s \\ D^0 & D^+ & D^+_s & \eta_c \end{pmatrix}, \tag{15}$$

The Feynman diagrams involved in the evaluation of the decay width of $R_{cc} \rightarrow DD^*$ are depicted in Fig. 4. They are similar to those of [37,38] since the transition $VV \rightarrow VP$ is also there. Essentially, we have two different structures which are depicted in Fig. 5. Diagram 1) contains a 3V- vertex and 2) has a PPV- vertex instead. Below, we evaluate both diagrams in Fig. 5.

3.1 Decay mediated by a vector meson, Fig. 5. 1)

To evaluate diagram 1), first we show the structures of the three different vertices that appear in Fig. 5, 1) (derived from Eq. (14)):

$$t_{RVV} = \frac{I g_R}{2} (\epsilon_1^i \epsilon_2^j - \epsilon_1^j \epsilon_2^i) \quad (16)$$

$$t_{V_3} = V_3 g \{ (2k + q - P)^\mu \epsilon_{(l)\nu} \epsilon_{2\mu} \epsilon_{(f)}^\nu - (k + P - q)^\mu \epsilon_{2\nu} \epsilon_{(l)\mu} \epsilon_{(f)}^\nu + (2(P - q) - k)_\mu \epsilon_{(l)\nu} \epsilon_{(f)}^\mu \epsilon_{2\nu}^\nu \} \quad (17)$$

$$t_{VVP} = A G' \epsilon^{\alpha\beta\gamma\delta} (P - q)_\alpha \epsilon_{2\beta} k_\gamma \epsilon_{(f)\delta} . \quad (18)$$

Here P is the total (initial) momentum of R_{cc} , k is the final momentum of the vector and q , the internal loop momentum, as assigned in Fig. 5. ϵ symbols with the indices 1, 2 and (l) , (f) are the polarization vectors of the resonance $R = R(1, 2)$, of the exchanged vector and the final vector meson respectively. After summing over polarizations,

$$\begin{aligned} \sum \epsilon_{1i} \epsilon_{1k} &= \delta_{ik} , \\ \sum \epsilon_{2j} \epsilon_{2l} &= \delta_{jl} , \end{aligned} \quad (19)$$

for the two-heavy and near-threshold $D_{(s)}^*$, and,

$$\sum \epsilon_{(l)\delta} \epsilon_{(l)\nu} = -g_{\delta\nu} + \frac{(P - k - q)_\delta (P - k - q)_\nu}{M_l^2} , \quad (20)$$

for the vector meson exchanged between V_1 and V_2 , hence, the amplitude can be written as,

$$\begin{aligned} -it^{ij} &= -\frac{1}{2} A I V_3 g_R G' g \int \frac{d^4 q}{(2\pi)^4} \frac{q_\alpha (P - k)_\gamma}{(q^2 - m_1^2)((P - q)^2 - m_2^2)((k + q - P)^2 - M_l^2)} \\ &\times \{ \epsilon_{(f)\delta} ((2k + q - P)^j \epsilon^{\alpha i \gamma \delta} - (2k + q - P)^i \epsilon^{\alpha j \gamma \delta} \\ &- (k + P)_\delta (\epsilon^{\alpha i \gamma \delta} \epsilon_{(f)}^j - \epsilon^{\alpha j \gamma \delta} \epsilon_{(f)}^i) \\ &+ (2(P - q) - k)_\mu \epsilon_{(f)}^\mu (\epsilon^{\alpha i \gamma j} - \epsilon^{\alpha j \gamma i}) \} . \end{aligned} \quad (21)$$

The second term is proportional to $(k_\gamma P_\delta - P_\gamma k_\delta) (\epsilon^{\alpha i \gamma \delta} \epsilon_{(f)}^j - \epsilon^{\alpha j \gamma \delta} \epsilon_{(f)}^i) = -2k_\gamma P_\delta (\epsilon^{\alpha i \gamma \delta} \epsilon_{(f)}^j - \epsilon^{\alpha j \gamma \delta} \epsilon_{(f)}^i)$. We apply a Feynman parametrization for this integral,

$$\frac{1}{abc} = 2 \int_0^1 dx \int_0^x dy \frac{1}{(a + (b - a)x + (c - b)y)^3} , \quad (22)$$

with

$$a = q^2 - m_1^2; \quad b = (P - q)^2 - m_2^2; \quad c = (P - q - k)^2 - M_l^2 . \quad (23)$$

Using the change of variable $q' = q - Px + ky$, it can be seen that the second term in Eq. (21) is proportional to

$$-2 \int_0^1 dx \int_0^x dy \int \frac{d^4 q'}{(2\pi)^4} \frac{(q' + Px - ky)_\alpha}{(q'^2 + s(M_l))^3} 2k_\gamma P_\delta (\epsilon^{\alpha i \gamma \delta} \epsilon_f^j - \epsilon^{\alpha j \gamma \delta} \epsilon_f^i), \quad (24)$$

with

$$s(M_l) = (P^2 - m_2^2 + m_1^2)x + (-2Pk - M_l^2 + m_2^2 + k^2)y - (Px - yk)^2 - m_1^2. \quad (25)$$

The term which is odd in q' vanishes and those not odd in q' are proportional either to $k_\gamma P_\delta P_\alpha \epsilon^{\alpha i \gamma \delta}$ or $k_\gamma P_\delta k_\alpha \epsilon^{\alpha i \gamma \delta}$, both being equal to zero. Hence, two different kinds of integral, which are parametrized using Lorentz covariance, remain in Eq. (21),

$$\begin{aligned} & \int \frac{d^4 q}{(2\pi)^4} \frac{q_\alpha (2k + q - P)_j}{(q^2 - m_1^2)((P - q)^2 - m_2^2)((k + q - P)^2 - M_l^2)} \\ &= i(aP_\alpha P_j + bP_\alpha k_j + ck_\alpha P_j + dk_\alpha k_j + eg_{\alpha j}) \\ & \int \frac{d^4 q}{(2\pi)^4} \frac{q_\alpha (2(P - q) - k)_\mu}{(q^2 - m_1^2)((P - q)^2 - m_2^2)((k + q - P)^2 - M_l^2)} \\ &= i(AP_\alpha P_\mu + BP_\alpha k_\mu + Ck_\alpha P_\mu + Dk_\alpha k_\mu + Eg_{\alpha\mu}) \end{aligned} \quad (26)$$

In Eq. (26), for $P_j = 0$ as in the center of mass system, only the terms proportional to b, d and e survives. Whereas when contracting with $\epsilon_{(f)}^\mu$ in the Lorentz gauge, terms with B and D are zero.

Let us start with the second integral. For convenience, we separate it into two terms, one that goes like $q_\alpha q_\mu$, and the other, proportional to q_α , with coefficients -2 and $(2P - k)^\mu$, respectively. We define,

$$\begin{aligned} & \int \frac{d^4 q}{(2\pi)^4} \frac{q_\alpha q_\mu}{(q^2 - m_1^2)((P - q)^2 - m_2^2)((k + q - P)^2 - M_l^2)} \\ &= i(A_1 P_\alpha P_\mu + B_1 P_\alpha k_\mu + C_1 k_\alpha P_\mu + D_1 k_\alpha k_\mu + E_1 g_{\alpha\mu}). \end{aligned} \quad (27)$$

For simplicity, we work in the center of mass system with the z axes defined in the direction of \vec{k} , the momenta of the final vector meson. Thus, we have, for the r. h. s. of Eq. (27),

- 1) For $\alpha = 0; \mu = 0$, $i(A_1 P_0^2 + B_1 P_0 k_0 + C_1 k_0 P_0 + D_1 k_0^2 + E_1)$,
- 2) For $\alpha = 0; \mu = 3$, $i(B_1 P_0 k_3 + D_1 k_0 k_3)$,
- 3) For $\alpha = 3; \mu = 3$, $i(D_1 k_3^2 - E_1)$.

Let us start with the second case of $\alpha = 0; \mu = 3$, where the integral of the l. h. s. of Eq. (27) is convergent. By taking the change of variable $q' = q - Px + ky$ and using the same

Feynman parametrization of Eqs. (22), (23) and (25), the integral is odd in q'_0 and/or q'_3 , and so we obtain,

$$B_1 = -\frac{1}{16\pi^2} \int_0^1 dx \int_0^x dy \frac{xy}{s(M_l) + i\epsilon}; \quad C_1 = B_1; \quad D_1 = \frac{1}{16\pi^2} \int_0^1 dx \int_0^x dy \frac{y^2}{s(M_l) + i\epsilon}, \quad (28)$$

where we have used the relation: $\int d^4q'/(q'^2 + s)^3 = i\pi^2/(2s)$.

Now inserting the coefficients of Eq. (28) in the resulting equation from Eq. (27) for each case, $\alpha = 0, \mu = 0$ and $\alpha = 3, \mu = 3$, we obtain the coefficients A_1 and E_1 ,

$$E_1 = \frac{i}{(2\pi)^3} f(P, k, M_l) + \frac{k_3^2}{16\pi^2} \int_0^1 dx \int_0^x dy \frac{y^2}{s(M_l) + i\epsilon}, \quad (29)$$

$$A_1 = \frac{1}{P_0^2} \left\{ -\frac{i}{(2\pi)^3} f_1(P, k, M_l) - \frac{1}{16\pi^2} \int_0^1 dx \int_0^x dy \frac{k_3^2 y^2 + k_0^2 y^2 - 2P_0 k_0 xy}{s(M_l) + i\epsilon} \right\}, \quad (30)$$

where

$$f(P, k, M_l) = \int \frac{dq^0 d\cos\theta dq q^4 \cos^2\theta}{(q^2 - m_1^2 + i\epsilon)((P - q)^2 - m_2^2 + i\epsilon)((k + q - P)^2 - M_l^2 + i\epsilon)} \quad (31)$$

$$f_1(P, k, M_l) = \int \frac{dq^0 d\cos\theta dq q^2 (q_0^2 + q^2 \cos^2\theta)}{(q^2 - m_1^2)((P - q)^2 - m_2^2)((k + q - P)^2 - M_l^2)}. \quad (32)$$

In the above equation we have performed the integral over the ϕ angle and $q_3 = q \cos\theta$, being θ the angle from the z axes. As can be observed, coefficients A_1 and E_1 contain logarithmically divergent integrals. To evaluate them, we perform the integral in q_0 , and then the integral over the three-momentum using a cutoff, q_{\max} . The choice of q_{\max} must be consistent with the maximum momenta needed in the two-meson loop integrals of the coupled-channel calculation, since here we have the same vertex of the resonance coupled to $D^* D_{(s)}^*$, as depicted in Fig. (3). In [23], the two-meson loop function is evaluated by means of the dimensional regularization, with $\mu = 1500$ MeV and $\alpha = -1.4$. We redo the coupled channel calculation in [23] using the formula for the two-meson loop function with cutoff, q_{\max} , which is,

$$G(s) = \frac{1}{4\pi^2} \int_0^{q_{\max}} q^2 dq \frac{\omega_1 + \omega_2}{\omega_1 \omega_2 (P_0^2 - (\omega_1 + \omega_2)^2 + i\epsilon)}, \quad (33)$$

Where $\omega_{1,2} = \sqrt{q^2 + m_{1,2}^2}$, and $m_{1,2} = m_{D^*}$ or $m_{D_s^*}$. We obtain the value of the cutoff needed to reproduce the states R_{cc} and S_{cc} in [23], $q_{\max} = 750$ MeV, and couplings slightly higher than in [23]: $g_R = 20895$ MeV and 14705 MeV for the R_{cc} and S_{cc} respectively.

In Eq. (26), the term not proportional to $q_\alpha q_\mu$ is convergent and can be evaluated by means of a Feynman parametrization. The explicit form of the integrals in Eqs. (31) and

(32) are given in the Appendix (A.2). Finally, the amplitude of the diagram in Fig. 5. 1), can be written as

$$t^{ij} = I g_X g A G' V_3 \epsilon_\delta \{ H P_\alpha k_\gamma (k^i \epsilon^{\alpha j \gamma \delta} - k^j \epsilon^{\alpha i \gamma \delta}) + F P_\gamma k_\alpha P^\delta \epsilon^{ij \gamma \alpha} - 3 e (P - k)_\gamma \epsilon^{ij \gamma \delta} \} , \quad (34)$$

with $H = (b + d)/2$ and $F = A + C$. The expressions of the coefficients that remain in Eq. (26) are given in the Appendix (A.2).

3.2 Decay mediated by a pseudoscalar meson, Fig. 5. 2)

Once we have evaluated the diagram in Fig. 5. 1), the one in Fig. 5. 2), with pseudoscalar exchange, is similarly obtained. From Eq. (14), the amplitude for the PPV vertex is

$$t_{PPV} = g P_V \epsilon_1^\mu (2(P - k) - q)_\mu . \quad (35)$$

Summing over polarizations of V_1, V_2 , $(\epsilon_{1i} \epsilon_{2j} - \epsilon_{1j} \epsilon_{2i}) \epsilon_{1k} \epsilon_{2l} = \delta_{ik} \delta_{jl} - \delta_{jk} \delta_{il}$, for the amplitude of the diagram in Fig. 5. 2), we obtain

$$-i t^{ij} = \frac{1}{2} g g_R G' A P_V I k_\gamma \epsilon_{(f) \delta} \int \frac{d^4 q}{(2\pi)^4} \frac{(P - q)^\alpha (\epsilon_\alpha^{j \gamma \delta} (2(P - k) - q)_i - \epsilon_\alpha^{i \gamma \delta} (2(P - k) - q)_j)}{((k - P + q)^2 - m_l^2 + i\epsilon)(q^2 - m_1^2)((P - q)^2 - m_2^2)} . \quad (36)$$

The integral in Eq. (36), without the antisymmetric tensor $\epsilon_\alpha^{j \gamma \delta}$ can be parametrized using Lorentz covariance as follows

$$\int \frac{d^4 q}{(2\pi)^4} \frac{(P - q)^\alpha (2(P - k) - q)^i}{((k - P + q)^2 - m_l^2 + i\epsilon)(q^2 - m_1^2 + i\epsilon)((P - q)^2 - m_2^2 + i\epsilon)} = i (\tilde{A} P^\alpha P^i + \tilde{B} P^\alpha k^i + \tilde{C} k^\alpha k^i + \tilde{D} k^\alpha P^i + \tilde{E} g^{\alpha i}) \quad (37)$$

The terms with the coefficients \tilde{A}, \tilde{D} are proportional to the momenta of the initial particle, $P^i = 0$, and the term that goes with \tilde{C} is zero since the presence of k_α makes $k_\alpha k_\gamma \epsilon^{\alpha i \gamma \delta} = 0$. Therefore, only \tilde{B} and \tilde{E} remain, and we obtain,

$$t^{ij} = \frac{1}{2} g_R (G' g) A P_V I k_\gamma \epsilon_{(f) \delta} \{ \tilde{B} P_\alpha (\epsilon^{\alpha i \gamma \delta} k^j - \epsilon^{\alpha j \gamma \delta} k^i) - 2 \tilde{E} \epsilon^{ij \gamma \delta} \} . \quad (38)$$

With \tilde{B} and \tilde{E} given in the Appendix (A.3).

3.3 Total amplitude and decay width

The sum of the amplitudes of the diagrams depicted in Fig. 5, including pseudoscalar and vector meson exchange, Eqs. (34) and (38), can be written as:

$$t_1^{ij} = g_R (G' g) \epsilon_{(f) \delta} \{ \mathcal{H} P_\alpha k_\gamma (k^i \epsilon^{\alpha j \gamma \delta} - k^j \epsilon^{\alpha i \gamma \delta}) + (\mathcal{I} k_\gamma + \mathcal{J} P_\gamma) \epsilon^{ij \gamma \delta} + \mathcal{F} P_\gamma k_\alpha P^\delta \epsilon^{ij \gamma \alpha} \} \quad (39)$$

with $\mathcal{H} = (\sum_{\text{diag}} (C_V H - \frac{1}{2} C_P \tilde{B}))$, $\mathcal{I} = (\sum_{\text{diag}} (3e(M_l)C_V - e(m_l)C_P))$, $\mathcal{J} = -\sum_{\text{diag}} 3e(M_l)C_V$, $\mathcal{F} = (\sum_{\text{diag}} C_V F)$, and $C_V = AIV_3$, $C_P = AIP_V$. The squared amplitud, $\sum_{\delta,i,j} |t_1^{ij}|^2$, is

$$\sum_{\delta} |t_1|^2 = g^2 g_X^2 G'^2 (r_1 |\vec{k}|^4 + r_2 |\vec{k}|^2 + r_3) \quad (40)$$

with

$$\begin{aligned} r_1 &= (2P_0^4 |\mathcal{F}|^2) / m_{V_f}^2 + 4P_0^2 |\mathcal{H}|^2, \\ r_2 &= 4|\mathcal{I}|^2 + (2P_0^2 |\mathcal{J}|^2) / m_{V_f}^2 + 4P_0^2 \text{Re}(\mathcal{I}\mathcal{F}^*) + (4k_0 P_0^3 \text{Re}(\mathcal{J}\mathcal{F}^*)) / m_{V_f}^2, \\ &\quad + 8k_0 P_0 \text{Re}(\mathcal{H}\mathcal{I}^*) + 8P_0^2 \text{Re}(\mathcal{H}\mathcal{J}^*), \\ r_3 &= 6m_{V_f}^2 |\mathcal{I}|^2 + 6P_0^2 |\mathcal{J}|^2 + 12k_0 P_0 \text{Re}(\mathcal{I}\mathcal{J}^*), \end{aligned} \quad (41)$$

where $m_{V_f} = m_{D^*}$. In practise, there is only one constant which is complex, \mathcal{I} for the diagram with $m_l = m_\pi$. The coefficients C_V and C_P needed in Eqs. (39) and (40) are giving in Tables 6 - 11. Finally, the decay width is given by:

$$\Gamma_{R_{cc} \rightarrow DD^*_{(s)}} = \frac{1}{2J+1} \frac{|\vec{k}| \sum_{\delta} |t_1|^2}{8\pi M_{R_{cc}}^2} \quad (42)$$

In Eq. (35), to reproduce the experimental decay width $D^{*+} \rightarrow D^0 \pi^+$, with $P_V = -1$, a value $g = g_D = 8.95$ is needed, which is significantly larger than that expected from SU(4), $g = 4.16$. However $(G'g)$, which is the factor that appears in the amplitude of the process $R_{cc} \rightarrow DD^*$, see Eq. (39), is not so different from what we expect from SU(4), because at the same time $\Gamma_{D^{*+} \rightarrow D^+ \gamma}^{\text{exp}}$ is smaller than what one obtains from the hidden gauge Lagrangian, and this can be compensated taking a value of G' smaller ($G' = 0.0087 \text{ MeV}^{-1}$ see section 5). Thus, we use the value of $(G'g) = 0.06 \text{ MeV}^{-1}$, obtained with $M_V = m_\rho$ and $f = f_\pi = 93 \text{ MeV}$, $g = M_V/2f$, and when performing the evaluation of the errors, we vary the $(G'g)$ constant from this value. Also, one must take into account that using this value of g , g_l or g_h , the subtraction constant α_h in [23] can be tuned to obtain the properly masses as explained in section 2.

4 Radiative decays of doubly charmed molecules into $DD\gamma$

In this section we consider the radiative decay of doubly charmed meson molecules, $R_{cc} \rightarrow DD\gamma$. In our picture, the decays occur via the one loop diagrams depicted in Fig. 6. Only non-vanishing diagrams are shown: the contact vertex $D^{*0} D^0 \gamma \pi^0$ leads to a zero amplitude (also, when the photon comes out from a neutral vector or pseudoscalar meson, the sum for all the intermediate neutral particles ρ , ω , J/ψ , gives zero. In the last two diagrams, 4) and 4.1), it is also possible to have the vertex $D^+ D^+ \gamma$ instead of $D^{*+} D^+ \gamma$. However, since

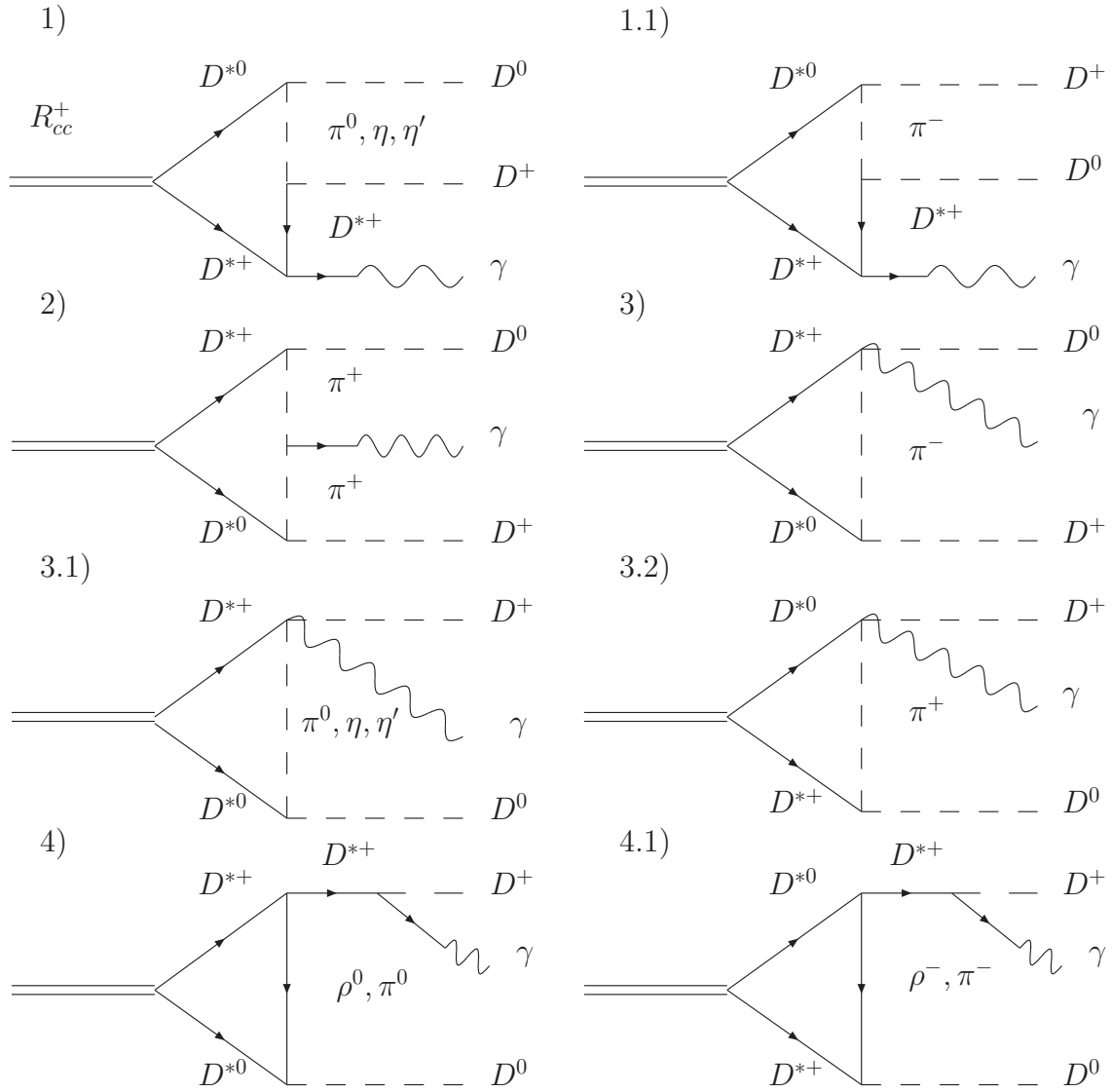


Figure 6: diagrams for the $R_{cc}^+ \rightarrow D^0 D^+ \gamma$ decay through one loop.

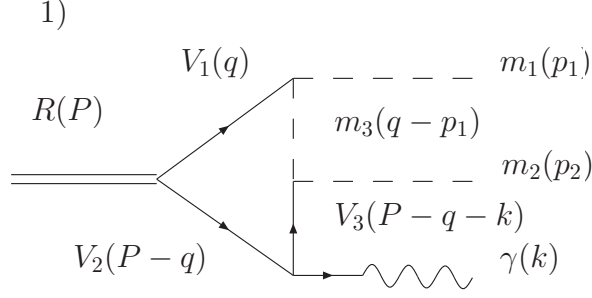


Figure 7: Momentum dependence of the first diagram in Fig. 6.

the initial state has $J^P = 1^+$, the intermediate transition $D^*D^* \rightarrow DD$ is not possible. Below, we evaluate the different structures 1), 2) and 3) depicted in Fig. 6. The decay width coming from diagrams 4) and 4.1) can be easily obtained from the evaluation of the decay width to $D_{(s)}D_{(s)}^*$ done in section 3, and their contributions is discussed in the Results section (6).

4.1 Evaluation of the diagram in Fig. 6 1).

To evaluate the diagram in Fig. 6 1), we show explicitly the momentum assignment in Fig. 7. The necessary interaction Lagrangians are given in Eq. (14). In addition, the hidden gauge Lagrangian, [8], provides the coupling of the vector meson dominance,

$$t_{V\gamma} = \mathcal{P}M_V^2 \frac{e}{g} \epsilon_{(\gamma)\alpha} \epsilon_V^\alpha. \quad (43)$$

Essentially, it replaces $\epsilon(V)$ by $\epsilon(\gamma)$ in Eq. (17). Then, we can write the amplitude as

$$\begin{aligned} -it_{ij}^1 &= \frac{1}{2} \mathcal{A} g^2 \tilde{g} e \epsilon_{(\gamma)\beta} \int \frac{d^4 q}{(2\pi)^4} (\epsilon_{1i} \epsilon_{2j} - \epsilon_{1j} \epsilon_{2i}) \epsilon_1^\mu \epsilon_3^{\mu'} (2p_1 - q)_\mu (p_1 - p_2 - q)_{\mu'} \\ &\times \left\{ \frac{(2k + q - P)_\alpha \epsilon_3^\beta \epsilon_2^\alpha}{1} - \frac{(k + P - q)_\alpha \epsilon_2^\beta \epsilon_3^\alpha}{1} + \frac{(2(P - q) - k)^\beta \epsilon_{\alpha 3} \epsilon_2^\alpha}{1} \right\} \\ &\times \frac{1}{(q - p_1)^2 - m_3^2} \frac{1}{q^2 - M_1^2} \frac{1}{(P - q)^2 - M_2^2} \frac{1}{(P - q - k)^2 - M_3^2}. \end{aligned} \quad (44)$$

with $\mathcal{A} = IV_3 \mathcal{P} P_V$. The sum over polarizations of vectors 1, 2, 3, gives,

$$\begin{aligned} \sum \epsilon_1^i \epsilon_1^\mu &\simeq -g^{i\mu} \\ \sum \epsilon_2^j \epsilon_2^\alpha &\simeq -g^{j\alpha} \\ \sum \epsilon_3^\beta \epsilon_3^{\mu'} &= -g^{\beta\mu'} + \frac{(P - q - k)^{\mu'} (P - q - k)^\beta}{m_3^2}. \end{aligned} \quad (45)$$

In the last sum in Eq. (45), it is possible to make an approximation without losing much in the numerical results. For the D^*D^* -molecule decaying into $DD\gamma$, the intermediate D^* of momentum $P-q-k$ is also close to mass-shell. In fact, when the photon takes its maximum energy, $E_\gamma^{\max} = (s - 4m_D^2)/2\sqrt{s}$, we have, for $\beta = \mu = 0$, $-1 + \frac{(P-q-k)^0(P-q-k)^0}{m_{D^*}^2} \simeq 0.23$ and for $\beta = 0$, $\mu = i$, $\frac{(P-q-k)^0(P-q-k)^i}{m_{D^*}^2} \simeq 0.1$. We make the approximation of neglecting the zero component of the last sum over polarizations in Eq. (45), which simplifies considerably the calculation. In this framework, the amplitude in Eq. (44) can be written as:

$$\begin{aligned}
-it_{ij}^1 &= \frac{1}{2} \mathcal{A} e g^2 \tilde{g} \epsilon_{(\gamma)m} \int \frac{d^4q}{(2\pi)^4} \frac{1}{(q-p_1)^2 - m_3^2} \frac{1}{q^2 - M_1^2} \frac{1}{(P-q)^2 - M_2^2} \\
&\times \frac{1}{(P-q-k)^2 - M_3^2} \{ (2p_1 - q)_i ((2k + q)_j (2p_1 + k - q)_m \\
&- (2p_1 + k - q)_l (k - q)_l \delta_{jm} + (-2q - k)_m (2p_1 + k - q)_j \\
&- (\text{same but } i \leftrightarrow j) \} .
\end{aligned} \tag{46}$$

The result of this integral, (without the factor $\frac{1}{2} \mathcal{A} e g^2 \tilde{g} \epsilon_{(\gamma)m}^m$) takes the form:

$$i(a_1(k_i \delta_{jm} - k_j \delta_{im}) + c_1(k_j p_{1i} p_{1m} - k_i p_{1j} p_{1m}) + d_1(p_{1i} \delta_{jm} - p_{1j} \delta_{im})) . \tag{47}$$

In the above expression, we have omitted the term $e_1(p_1^i k^j k^m - p_1^j k^i k^m)$, which disappears when contracting with $\epsilon_{(\gamma)}^m$ in the Coulomb gauge. The integral in Eq. (46) is convergent and we use the formula for the Feynman parametrization for $n = 4$ to evaluate it,

$$\frac{1}{abcd} = 6 \int_0^1 dx \int_0^x dy \int_0^y \frac{dz}{(a + (b-a)x + (c-b)y + (d-c)z)^4} \tag{48}$$

with

$$\begin{aligned}
a &= q^2 - M_1^2 \\
b &= (q - p_1)^2 - m_3^2 \\
c &= (P - q)^2 - M_2^2 \\
d &= (P - q - k)^2 - M_3^2 .
\end{aligned} \tag{49}$$

The change of variable, $q = q' + p_1 x + (P - p_1)y - kz$, simplifies the denominator in Eq. (48) as $(q'^2 + s)^4$ with

$$\begin{aligned}
s &= (p_1^2 + M_1^2 - m_3^2)x + (P^2 - M_2^2 - p_1^2 + m_3^2)y + (-2Pk - M_3^2 + M_2^2)z \\
&- M_1^2 - (p_1 x + (P - p_1)y - kz)^2 .
\end{aligned} \tag{50}$$

Picking up the coefficients of $k_i \delta_{mj}$, $k_j p_{1i} p_{1\beta}$, $p_{1i} \delta_{mj}$, keeping the antisymmetric combination in the indices i, j , we obtain,

$$t_{ij}^1 = -\frac{1}{2} \mathcal{A} e g^2 \tilde{g} \epsilon_{(\gamma)m} (a_1(k_i \delta_{jm} - k_j \delta_{im}) + c_1(k_j p_{1i} p_{1m} - k_i p_{1j} p_{1m}) + d_1(p_{1i} \delta_{jm} - p_{1j} \delta_{im})) , \tag{51}$$

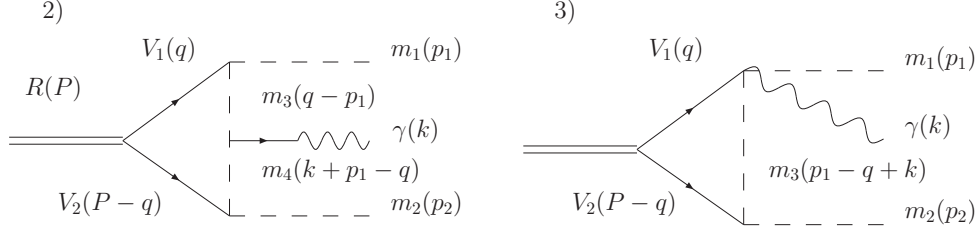


Figure 8: Momentum dependence of the Feynman diagrams type 2) and 3) in Fig. 6.

And the coefficients a_1 , c_1 and d_1 are given in the Appendix (A.4).

4.2 Evaluation of diagrams Fig. 6 2) and 3).

Let us consider the relevant diagrams in Fig. 8, with momentum variables shown explicitly. For diagram 2), the amplitude is:

$$\begin{aligned}
 -it_{ij}^{(2)} = & \frac{1}{2} \mathcal{B} e g^2 \tilde{g} \epsilon_{(\gamma)}^\alpha \int \frac{d^4 q}{(2\pi)^4} \frac{1}{q^2 - M_1^2} \frac{1}{(q - p_1)^2 - m_3^2} \frac{1}{(p_1 + k - q)^2 - m_4^2} \frac{1}{(P - q)^2 - M_2^2} \\
 & \times (2(q - p_1) - k)_\alpha \{ (2p_1 - q)_i (p_1 - p_2 + k - q)_j - (2p_1 - q)_j (p_1 - p_2 + k - q)_i \}
 \end{aligned} \quad (52)$$

with $\mathcal{B} = IP P_V$, and $P_V = P_{V_1} P_{V_2} P_{V_3}$ (the product of the coefficients for the PPV vertices in Eq. (35)). The integral in Eq. (52) must be like:

$$i(a_2(k_i g_{\alpha j} - k_j g_{\alpha i}) + b_2 P_\alpha (p_{1i} k_j - k_i p_{1j}) + c_2(k_j p_{1i} - k_i p_{1j}) p_{1\alpha} + d_2(p_{1i} g_{\alpha j} - p_{1j} g_{\alpha i})) . \quad (53)$$

We apply the change of variable $q = q' + (P - p_1)y + (p_1 - P + k)z$ with the same Feynman parametrization of Eq. (48), but now $d = (p_1 - q + k)^2 - m_4^2$. In the Coulomb gauge for the polarization vector of the photon, we can take $\epsilon_{(\gamma)}^0 = 0$ and $\epsilon_{(\gamma)}^i k_i = 0$, we can neglect the second term. We obtain,

$$t_{ij}^{(2)} = -\frac{1}{2} \mathcal{B} e g^2 \tilde{g} \epsilon_{(\gamma) m} (a_2(k_i \delta_{mj} - k_j \delta_{mi}) - c_2(k_j p_{1i} - k_i p_{1j}) p_{1m} + d_2(p_{1i} \delta_{mj} - p_{1j} \delta_{mi})) , \quad (54)$$

which has the same form than Eq. (51). The coefficients a_2 , c_2 and d_2 are given in the Appendix (A.4).

To evaluate the diagram in Fig. 6 3), we use the Lagrangian [8]

$$\mathcal{L}_{V\gamma PP} = \frac{e M_V^2}{4g f^2} A_\mu \langle V^\mu (Q\Phi^2 + \Phi^2 Q - 2\Phi Q\Phi) \rangle , \quad (55)$$

for the $V\gamma PP$ vertex, with $Q = \frac{1}{3} \text{diag}(2, -1, -1, 2)$, which leads to

$$t_{V\gamma PP} = V_{2P\gamma} \epsilon_{(\gamma) \nu}^\nu . \quad (56)$$

Thus the amplitude of diagram Fig. 8 3) is

$$t_{ij}^3) = -\frac{1}{2}\mathcal{C}eg^2\tilde{g}\epsilon_{(\gamma)m}a_3((k_i\delta_{mj} - k_j\delta_{mi}) + (p_{1i}\delta_{mj} - p_{1j}\delta_{mi})) \quad (57)$$

where $\mathcal{C} = IP_{V_1}V_{2P\gamma}$ and a_3 is given in the Appendix (A.4).

4.3 Total amplitude

So far we have seen that the amplitude takes the structure of Eq. (51) with the coefficients contributed from various diagrams. Therefore, the square amplitude takes the following form with the coefficients computed from Eqs. (51), (54) and (57)

$$\begin{aligned} \sum_{\delta ij} |t_{2ij}|^2 &= \frac{1}{4} \frac{eg^2\tilde{g}}{|\vec{k}|^2} (2(C^2 f(\vec{k}, \vec{p}_1)^2 + 2AC f(\vec{k}, \vec{p}_1) \vec{k}^2 + 2A^2 \vec{k}^4 + 2D \vec{k} \cdot \vec{p}_1 (C f(\vec{k}, \vec{p}_1) + 2A \vec{k}^2) \\ &+ D^2 (f(\vec{k}, \vec{p}_1) + 2\vec{k}^2 \vec{p}_1^2))) \end{aligned} \quad (58)$$

with

$$f(\vec{k}, \vec{p}_1) = (\vec{k} \cdot \vec{p}_1)^2 - |\vec{k}|^2 |\vec{p}_1|^2 \quad (59)$$

and

$$\begin{aligned} A &= \mathcal{A}a_1 + \mathcal{B}a_2 + \mathcal{C}a_3 \\ C &= \mathcal{A}c_1 - \mathcal{B}c_2 \\ D &= \mathcal{A}d_1 + \mathcal{B}d_2 + \mathcal{C}a_3 . \end{aligned} \quad (60)$$

In addition, if we call p_1 to the momenta of the D^0 in the final state, in order to consider all diagrams in Fig. 6 including those where it is placed D^+ with momenta p_2 instead of D^0 (diagrams of Fig. 6 1.1), 3.1) and 3.2)) we do in Eq. (58),

$$\begin{aligned} A &\rightarrow A + A' - D' \\ C &\rightarrow C + C' \\ D &\rightarrow D - D' , \end{aligned} \quad (61)$$

where A , C and D of the r. h. s of Eq. (61) are those coefficients in Eq. (60) and A' , C' , D' , the same but changing $p_1 \rightarrow p_2 = P - p_1 - k$ and $p_2 \rightarrow p_1$.

The final decay width of the process $R_{cc}^+(P) \rightarrow D^0(p_1)D^+(p_2)\gamma(k)$ for the initial particle at rest, is

$$\begin{aligned} \Gamma &= \frac{1}{64M_X\pi^3(2J+1)} \int_{E_{1\min}}^{E_{1\max}} dE_1 \int_{E_{\gamma\min}}^{E_{\gamma\max}} dE_\gamma \theta(1 - \cos^2\theta) \sum_{\delta} |t_2|^2 , \text{ with} \\ \cos\theta &= \frac{(M_X - E_1 - E_\gamma)^2 - m_2^2 - |\vec{p}_1|^2 - |\vec{k}|^2}{2|\vec{p}_1||\vec{k}|} \\ E_{1\min} &= m_1 , E_{2\max} = \frac{s + m_1^2 - m_2^2}{2\sqrt{s}} \\ E_{\gamma\min} &= 0 , E_{\gamma\max} = \frac{s - m_1^2 - m_2^2 - 2m_1m_2}{2\sqrt{s}} , \end{aligned} \quad (62)$$

being θ the angle between p_1 and k .

5 Decay of doubly charmed state to $D^*D\gamma$

Finally, we consider the radiative decay depicted in Fig. 9. In order to evaluate both diagrams for $R_{cc}^+ \rightarrow D^{*0}D^+\gamma$ and $R_{cc}^+ \rightarrow D^{*+}D^0\gamma$, we need the amplitude for the decay $D^{*+} \rightarrow D^+\gamma$ and $D^{*0} \rightarrow D^0\gamma$. They are given by the Lagrangian in Eq. (14), and the amplitude is

$$t_{(D^* \rightarrow D\gamma)} = -\frac{G'}{\sqrt{2}g} e C' q_\mu \epsilon_{(D^{*+})\nu} k_\alpha \epsilon_{(\gamma)\beta} \epsilon^{\mu\nu\alpha\beta} \text{ with } C' = \begin{cases} \frac{4}{3} \text{ for } D^{*0} \\ \frac{1}{3} \text{ for } D^{*+} \\ \frac{1}{3} \text{ for } D_s^{*+} \end{cases} \quad (63)$$

Fixing the coupling $g = m_\rho/2f_\pi = 4.16$, we can use a value of G' in order to reproduce the experimental decay widths from the PDG, which is $\Gamma(D^{*+} \rightarrow D^+\gamma)/\Gamma_{D^{*+}} = (1.6 \pm 0.4)\%$, with $\Gamma_{D^{*+}} = 96 \pm 22$ KeV. We obtain $G' = 0.0087$ MeV⁻¹.

Now the amplitude of the processes depicted in Fig. 9,

$$t_{3ij} = I g_R \frac{1}{2} \frac{G'}{\sqrt{2}g} e C' \frac{1}{q^2 - m_{D^*}^2} q_\mu k_\alpha \epsilon_{(\gamma)\beta} \left(\epsilon_j^{\mu\alpha\beta} \epsilon_{1i} - \epsilon_i^{\mu\alpha\beta} \epsilon_{1j} \right). \quad (64)$$

Taking the square of this, we find the decay width

$$\Gamma = \frac{1}{32 M_R \pi^3} \int \frac{\tilde{p}_2 p_1}{\sqrt{s}} \frac{1}{2J+1} \sum_\delta |t_3|^2 dM_{D\gamma} \quad (65)$$

$$(66)$$

with

$$\sum_\delta |t_3|^2 = -\frac{C'^2 I^2 g_R^2 G'^2 e^2}{4g^2} \left(\frac{M_{D\gamma}^2 - m_D^2}{M_{D\gamma}^2 - m_{D^*}^2} \right)^2 \quad (67)$$

and

$$\text{and } \tilde{p}_2 = \frac{\lambda^{1/2}(M_{D\gamma}^2, 0, m_D^2)}{2 M_{D\gamma}}, p_1 = \frac{\lambda^{1/2}(M_R^2, m_D^2, M_{D\gamma}^2)}{2 M_R}.$$

where $M_{D\gamma}$ is the invariant mass of the D meson and γ .

6 Results

In this section we discuss the numerical results of the decays evaluated in the previous sections. They are shown in Table 2. Here, Γ_{tot} is the full width, Γ^k are the partial decay widths for the two possible channels $k = 1, 2$, ex. D^0D^{*+} and D^+D^{*0} , and Γ_j^k is

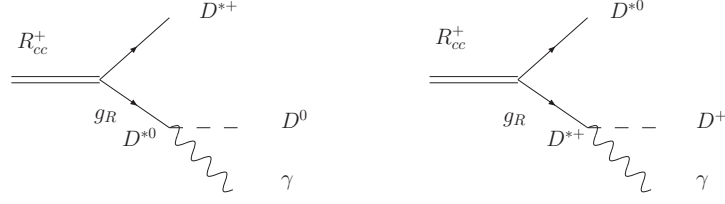


Figure 9: Decay of the doubly charmed states into $D^*D_{(s)}\gamma$

$\Gamma_{R(S)\rightarrow D_{(s)}D\pi} = \Gamma^k \Gamma_{D^*\rightarrow D\pi}/\Gamma_{D^*}$ (*hadronic decays*) or $\Gamma_{R(S)\rightarrow DD_{(s)}\gamma} = \Gamma^k \Gamma_{D_{(s)}^*\rightarrow D_{(s)}\gamma}/\Gamma_{D_{(s)}^*}$ (*radiative decays*). The partial decay widths of D^* and D_s^* to $D\pi$ and $D_{(s)}\gamma$, are taken from the PDG. The error shown is evaluated combining both, theoretical and the experimental errors from PDG.

To evaluate the errors we have considered variations of all parameters involved in the calculation. However some of them are not independent, and the evaluation of the error has to be done carefully. In the case of the decay into $DD_{(s)}^*$, we have the following parameters: (gG') , q_{\max} and g_R . As mentioned, the coupling of the resonance, g_R to the $D^*D_{(s)}^*$ and q_{\max} are not independent. Furthermore, the mass of the states that we have found at $M_R = 3970$ MeV and 4100 MeV also depends on q_{\max} : the bigger the cutoff is, the more bound the obtained state is, and the coupling g_R also grows. Thus, the main source of uncertainties come from variations in the parameters (gG') and q_{\max} . Performing the coupled channel calculation for several q_{\max} around 750 MeV, using linear regression we have found the following approximated relations valid close to the masses of the resonances $R_c(S_c)$, between the binding energy, B , defined as $B = \sqrt{s_{th}} - M_R$, q_{\max} and g_R :

$$\begin{aligned} B_1 &= -110 + 0.21 q_{\max}; & g_{1,R} &= -929 + 28 q_{\max} \text{ for } R_{cc}(3970) \\ B_2 &= -88 + 0.144 q_{\max}; & g_{2,R} &= -13216 + 37 q_{\max} \text{ for } S_{cc}(4100), \end{aligned} \quad (68)$$

for $i = 1, 2$, the doubly charmed states without and with strangeness respectively. Taking a gaussian distribution around the mean values of (gG') and q_{\max} with $\sigma = 0.15\mu$, and using the above relations, we obtain the errors shown in Table 2.

We observe that the total widths of the doubly charmed states, which comes basically from the decay into D^0D^{*+} and D^+D^{*0} for the R_{cc}^+ , from the channels $D^0D_s^{*+}$ and $D_s^+D^{*0}$ for the S_{cc}^+ , $D_s^+D^{*+}$ and $D^+D_s^{*+}$ for the S_{cc}^{++} , are (44 ± 12) , (24 ± 8) , and (24 ± 8) MeV for the R_{cc}^+ , S_{cc}^+ and S_{cc}^{++} respectively, giving both channels (ex. D^0D^{*+} and D^+D^{*0}) the same contribution to the width.

The direct diagrams with three/four propagators of Fig. 6, type 1), 2) and 3), lead to a very small width of the order of few KeV in the case of the $R_{cc}^+(3970)$ and $S_{cc}^+(4100)$ and 0.13 KeV for the doubly charge state, $S_{cc}^{++}(4100)$, the difference in one order of magnitude is due to the lack of type 2) diagram in this case. The $D^*D_{(s)}\gamma$ decay channel is smaller than 1 KeV, except for the channel $D_s^{*+}D^0\gamma$ channel of the R_{cc}^+ state, which is 4 KeV. Direct diagrams with four propagators like in Fig. 6, type 1), substituting the final vector

line by a pseudoscalar, would also be possible for $DD_{(s)}\pi$ in the final state, however, they have anomalous couplings together with heavy meson propagator, for what we expect them to be also very small.

Thus, the diagrams responsible of the radiative decay of the doubly charmed molecules are those of type 4) in Fig. 6, where the photon comes out from a D^* meson. The width from these diagrams is obtained from section 3, multiplying Γ^k , the width of $R_{cc} \rightarrow DD^*$ by $\Gamma_{D^* \rightarrow D\gamma}/\Gamma_{D^*}$, the last quantity taken from the PDG.

Therefore, the most important decay modes of the doubly charmed mesons are $DD\pi$, $DD\gamma$, where $D\pi$ and $D\gamma$ comes from the decay of D^* , and $DD_s\pi$, $DD_s\gamma$, for the strangeness ones.

Finally, we perform the evaluation of the $R_{cc} \rightarrow DD^*$ decay width, shown in Fig. 4, for only one meson exchanged, π , ρ , The result is shown in Table 3 for each doubly charmed meson. We can see that the most important contribution comes from ρ exchange, then π and ω respectively for the $R_{cc}^+(3970)$, where the interaction of the ρ and π are constructive, and opposite sign for the ω . For the $S_{cc}(4100)^{++}$, the most important contribution comes from the K^* , then, K and J/ψ , being the J/ψ exchange of opposite sign than the K^* , K .

7 Conclusions

We have considered the possible decay modes of the doubly charmed molecules of [23], $R_{cc}^+(3970)$, $S_{cc}^+(4100)$ and $S_{cc}^{++}(4100)$, and evaluated partial decay widths to $DD_{(s)}\pi$ and $DD_{(s)}\gamma$. We find that the main source of these decays come from the decay of a $D_{(s)}^*$ meson into $D_{(s)}\pi$ or $D_{(s)}\gamma$. The total widths of the doubly charmed molecules are 44 ± 12 MeV for the $R_{cc}^+(3970)$ and 24 ± 8 MeV for the $S_{cc}^+(4100)$ and $S_{cc}^{++}(4100)$. These decays are mediated by the exchange of one meson, vector or pseudoscalar, between the $D^*D_{(s)}^*$ pair of the molecule. The largest width comes from ρ , π and ω exchange for the $R_{cc}(3970)$, and K^* , K , J/ψ exchange for the $S_{cc}(4100)$.

These mesons are under challenge for experiments, since they are not $q\bar{q}$, having a pair of cc and doubly charged. How to produce these mesons is a difficult question. Up to now, the only observed doubly charmed particle is the Ξ_{cc}^+ , by its decays, $\Lambda^+K^-\pi^+$ and pD^+K^- [39], however, the BABAR experiment didn't find evidence for a Ξ_{cc}^+ in a search in $\Lambda_c^+K\pi^+$ and $\Xi_c^0\pi^+$ modes [40]. The same for the BELLE experiment, without any evidence for a Ξ_{cc}^+ in the $\Lambda_c^+K^-\pi^+$ mode [41]. In the case of e^+e^- collisions, Belle has produced double charmed quarks in the final state, $J/\psi + c\bar{c}$, however the cross section is very small $\sigma(e^+e^- \rightarrow J/\psi + c\bar{c}) = (0.74 \pm 0.08)$ pb and $J/\psi X_{\text{non}c\bar{c}}$ cross section is $(0.43 \pm 0.09 \pm 0.09)$ pb [42], not being able to produce the $c\bar{c}$ pair without J/ψ in the final state. More likely, they could be observed by the LHC in pp collisions or in JPARC, and being fortunated, the experimentalist could find both, the missed doubly charmed baryon and meson.

<i>State</i>	<i>Channel k</i>	Γ^k [MeV]	<i>Channel j</i>	Γ_j^k [MeV]	Γ_{tot} [MeV]
$R_{cc}^+(3970)$	<i>Hadronic decays</i>				
	$D^0 D^{*+}$	22 ± 6	$D^0(D^+\pi^0)$	7 ± 2	44 ± 12
			$D^0(D^0\pi^+)$	15 ± 4	
	$D^+ D^{*0}$	22 ± 6	$D^+(D^0\pi^0)$	14 ± 4	
	<i>Radiative decays</i>				
	$D^+ D^{*0}$		$D^+(D^0\gamma)$	8 ± 2	
	$D^0 D^{*+}$		$D^0(D^+\gamma)$	0.4 ± 0.2	
			$D^0 D^+\gamma$	$(2 \pm 1) \times 10^{-3}$	
			$D^{*0} D^+\gamma$	$(0.03 \pm 0.01) \times 10^{-3}$	
			$D^{*+} D^0\gamma$	$(0.5 \pm 0.2) \times 10^{-3}$	
$S_{cc}^+(4100)$	<i>Hadronic decays</i>				
	$D_s^+ D^{*0}$	12 ± 4	$D_s^+(D^0\pi^0)$	7 ± 2	24 ± 8
	$D^0 D_s^{*+}$	12 ± 4	-	-	
	<i>Radiative decays</i>				
	$D^0 D_s^{*+}$		$D^0(D_s^+\gamma)$	11 ± 4	
	$D_s^+ D^{*0}$		$D_s^+(D^0\gamma)$	5 ± 2	
			$D^0 D_s^+\gamma$	$(2 \pm 1) \times 10^{-3}$	
			$D^{*0} D_s^+\gamma$	$(0.3 \pm 0.1) \times 10^{-3}$	
			$D_s^{*+} D^0\gamma$	$(4 \pm 1) \times 10^{-3}$	
	$S_{cc}^{++}(4100)$	<i>Hadronic decays</i>			
$D_s^+ D^{*+}$		12 ± 4	$D_s^+(D^+\pi^0)$	4 ± 1	24 ± 8
			$D_s^+(D^0\pi^+)$	8 ± 3	
$D^+ D_s^{*+}$		12 ± 4	-	-	
<i>Radiative decays</i>					
$D^+ D_s^{*+}$			$D^+(D_s^+\gamma)$	11 ± 4	
$D_s^+ D^{*+}$			$D_s^+(D^+\gamma)$	0.2 ± 0.1	
			$D^+ D_s^+\gamma$	$(1.3 \pm 0.1) \times 10^{-4}$	
			$D^{*+} D_s^+\gamma$	$(0.3 \pm 0.1) \times 10^{-3}$	
			$D_s^{*+} D^+\gamma$	$(0.3 \pm 0.1) \times 10^{-3}$	

Table 2: Total and partial decay widths of the different decay modes of the doubly charmed states.

<i>State</i>	<i>Intermediate meson</i>	Γ_k [MeV]
$R_{cc}^+(3970)$	ρ	15.2
	π	7.2
	ω	1.7
	J/ψ	0.6
	η	0.14
	η_c	0.07
	η'	0.018
	$\rho + \pi$	30.0
	$\rho + \omega$	7.0
	$\pi + \omega$	6.0
$S_{cc}^{+(+)}(4100)$	K^*	15.0
	K	4.3
	J/ψ	1.7
	η	0.4
	η'	0.2
	η_c	0.19
		$K^* + K$
	$K^* + J/\psi$	9.8
	$J/\psi + K$	4.2

Table 3: Decay width obtained from the diagrams in Fig. 6 for one meson exchanged.

A Appendix

A.1 Pole positions of the dynamically generated XYZ using two different prescriptions for $g = m_V/(2f)$ in Eqs. (5) and (6).

The pole positions and coupling constants in the hidden charm sector using $\alpha_h = -1.4$ and $g_l = m_\rho/(2f_\pi)$ or $\alpha_h = -1.27$ and $g_h = m_{D^*}/(2f_D)$ in the $H - H$ channels. As one can observe, the use of a different strength g_h for these channels is compensated by small changes in α_h and the strongest coupling to the main channel, $D^*\bar{D}^*$ or $D_s^*\bar{D}_s^*$ barely changes.

	$ g_R [\text{MeV}]$			(g_l)
$\sqrt{s_0}[\text{MeV}]$	$3936 + i 6$	$3940 + i 0.0$	$3921 + i 30$	$4174 + i 97$
$\alpha_h = -1.4$	$I = 0; J = 0$	$I = 0; J = 1$	$I = 0; J = 2$	$I = 0; J = 2$
$D^* \bar{D}^*$	18700	18260	20600	2250
$D_s^* \bar{D}_s^*$	9900	9900	9050	20400
$K^* \bar{K}^*$	4	40	10	100
$\rho\rho$	50	0	100	90
$\omega\omega$	1400	0	2800	2970
$\phi\phi$	710	0	1600	3800
$J/\psi J/\psi$	390	0	2400	2400
$\omega J/\psi$	1600	0	4500	3400
$\phi J/\psi$	490	0	1900	6900
$\omega\phi$	60	0	190	2100
	$ g_R [\text{MeV}]$			(g_h)
$\sqrt{s_0}[\text{MeV}]$	$3950 + i 12$	$3955 + i 0.0$	$3922 + i 24$	$4161 + i 50$
$\alpha_h = -1.27$	$I = 0; J = 0$	$I = 0; J = 1$	$I = 0; J = 2$	$I = 0; J = 2$
$D^* \bar{D}^*$	18000	17200	21000	900
$D_s^* \bar{D}_s^*$	10500	11000	5200	19500
$K^* \bar{K}^*$	30	80	50	90
$\rho\rho$	60	0	80	50
$\omega\omega$	1700	0	2300	1700
$\phi\phi$	1400	0	1800	2800
$J/\psi J/\psi$	390	0	3200	4450
$\omega J/\psi$	1700	0	3500	1800
$\phi J/\psi$	1400	0	2800	5500
$\omega\phi$	440	0	830	1900

Table 4: Pole positions and couplings g_R to the different channels in two cases 1) using $g = m_\rho/(2f_\pi)$ in all channels, or 2) use of $g_h = m_{D^*}/(2f_D)$ in the channels where heavy mesons are involved, for Isospin= 0.

	$ g_R [\text{MeV}]$	
$\sqrt{s_0}[\text{MeV}]$	$3969 + i 140$	$3924 + i 70$
$I = 1; J = 2$	(g_l)	(g_h)
$D^* \bar{D}^*$	20500	20560
$K^* \bar{K}^*$	190	150
$\rho\rho$	0	0
$\rho\omega$	5000	3600
$\rho J/\psi$	8700	6200
$\rho\phi$	3700	2600

Table 5: Pole positions and couplings g_R to the different channels in two cases 1) using $g = m_\rho/(2f_\pi)$ in all channels, or 2) use of $g_h = m_{D^*}/(2f_D)$ in the channels where heavy mesons are involved, for Isospin= 1.

A.2 Decay of $R_c(S_c)$ to DD^* : Coefficients in Eq. (26).

The coefficients that survives in Eq. (26),

$$\begin{aligned}
b &= \frac{1}{16\pi^2} \int_0^1 dx \int_0^x dy \frac{(2-y)x}{s(M_l) + i\epsilon} \\
d &= \frac{1}{16\pi^2} \int_0^1 dx \int_0^x dy \frac{(y-2)y}{s(M_l) + i\epsilon} \\
e &= \frac{i}{(2\pi)^3} f(P, k, M_l) + \frac{k_3^2}{16\pi^2} \int_0^1 dx \int_0^x dy \frac{y^2}{s(M_l) + i\epsilon} \\
A &= \frac{1}{P_0^2} \left\{ \frac{2i}{(2\pi)^3} f_1(P, k, M_l) + \frac{1}{8\pi^2} \int_0^1 dx \int_0^x dy \frac{k_3^2 y^2 + k_0^2 y^2 - 2P_0 k_0 xy + x P_0^2}{s(M_l) + i\epsilon} \right\} \\
C &= \frac{1}{8\pi^2} \int_0^1 dx \int_0^x dy \frac{(x-1)y}{s(M_l) + i\epsilon} \\
E &= -2e(M_l) ,
\end{aligned} \tag{69}$$

with

$$s(M_l) = (P^2 - m_2^2 + m_1^2)x + (-2Pk - M_l^2 + m_2^2 + k^2)y - (Px - yk)^2 - m_1^2 . \tag{70}$$

The integrals in Eqs. (31), (32), and (69),

$$\begin{aligned}
f(P, k, M_l) &= \int \frac{dq_0 dq dx q^4 x^2}{(q^2 - M_1^2 + i\epsilon)((P-q)^2 - M_2^2 + i\epsilon)((P-q-k)^2 - M_l^2 + i\epsilon)} \\
&= -i2\pi \int_0^{q_{\max}} dq \int_{-1}^1 dx q^4 x^2 \times
\end{aligned}$$

$$\begin{aligned}
& \times \left(\frac{1}{2\omega_1(P_0 - \omega_1 + \omega_2 - i\epsilon)(P_0 - \omega_1 - \omega_2 + i\epsilon)(k^0 - P^0 + \omega_1 - \omega_l + i\epsilon)(k^0 - P^0 + \omega_1 + \omega_l - i\epsilon)} \right. \\
& \times \frac{1}{2\omega_2(P_0 - \omega_1 + \omega_2 + i\epsilon)(P_0 + \omega_1 + \omega_2 - i\epsilon)(k^0 + \omega_2 - \omega_l + i\epsilon)(k^0 + \omega_2 + \omega_l - i\epsilon)} \\
& \left. \times \frac{1}{2\omega_l(P_0 - k_0 + \omega_1 + \omega_l - i\epsilon)(P_0 - k_0 - \omega_1 + \omega_l + i\epsilon)(k^0 + \omega_2 - \omega_l - i\epsilon)(k^0 - \omega_2 - \omega_l + i\epsilon)} \right) \quad (71)
\end{aligned}$$

$$\begin{aligned}
f_1(P, k, M_l) &= \int \frac{dq_0 dq dx q^2 (q_0^2 + q^2 x^2)}{(q^2 - m_1^2)((P - q)^2 - m_2^2)((k + q - P)^2 - M_l^2)} \\
&= -i\pi \int_{-1}^1 dx \int_0^{q_{\max}} q^2 dq \times \\
& \times \left(\frac{q^2 x^2 + \omega_1^2}{\omega_1(i\epsilon + P_0 - \omega_1 - \omega_2)(-i\epsilon + P_0 - \omega_1 + \omega_2)(i\epsilon + P_0 - k_0 - \omega_1 - \omega_l)(-i\epsilon + P_0 - k_0 - \omega_l + \omega_1)} \right. \\
& \quad \left. - \frac{-P_0^2 - q^2 x^2 - 2P_0\omega_2 - \omega_2^2}{(-i\epsilon - P_0 + \omega_1 - \omega_2)\omega_2(P_0 + \omega_1 + \omega_2)(-i\epsilon - k_0 - \omega_2 + \omega_l)(k_0 + \omega_2 + \omega_l)} \right. \\
& \quad \left. - \frac{-P_0^2 - q^2 x^2 - k_0^2 - 2P_0\omega_l - \omega_l^2 + 2k_0(P_0 + \omega_l)}{(i\epsilon - P_0 + k_0 - \omega_1 - \omega_l)(-i\epsilon - P_0 + k_0 + \omega_1 - \omega_l)(i\epsilon + k_0 - \omega_2 - \omega_l)(-i\epsilon + k_0 + \omega_2 - \omega_l)\omega_l} \right) \quad (72)
\end{aligned}$$

with $\omega_{1,2} = \sqrt{q^2 + m_{1,2}^2}$, $\omega_l = \sqrt{q^2 + |\vec{k}|^2 + 2q|\vec{k}|x + M_l^2}$ and $x = \cos\theta$.

The coefficients in Eq. (38),

$$\begin{aligned}
\tilde{B} &= \frac{1}{16\pi^2} \int_0^1 dx \int_0^x dy \frac{(x-1)(2-y)}{s(m_l) + i\epsilon} \\
\tilde{E} &= e(m_l) \quad (73)
\end{aligned}$$

Where $e(m_l)$ and $s(m_l)$ stands for e and s in the formulas of Eqs. (69) and (70), but the mass of the vector meson exchanged, M_l , replaced by the pseudoscalar one, m_l .

A.3 Direct decays of $R_c(S_c)$ into $DD\gamma$: coefficients for the amplitudes from the Feynmann diagrams depicted in Fig. 6 1), 2) and 3).

The coefficients in Eq. (51),

$$\begin{aligned}
a_1 &= -i6 \int_0^1 dx \int_0^x dy \int_0^y dz \frac{d^4 q'}{(2\pi)^4} \frac{a_1^b \vec{q}'^2 + a_1^c}{(q'^2 + s)^4} = \frac{1}{32\pi^2} \int_0^1 dx \int_0^x dy \int_0^y dz \left(\frac{-3a_1^b}{s} + \frac{2a_1^c}{s^2} \right), \\
a_1^b &= -2 - \frac{5z}{3},
\end{aligned}$$

$$a_1^c = -z(-2(-1+x-y)(1+z)\vec{k} \cdot \vec{p}_1 + (x^2 - 2x(1+y) + y(2+y))\vec{p}_1^2) , \quad (74)$$

$$c_1 = -i6 \int_0^1 dx \int_0^x dy \int_0^y dz \frac{d^4 q'}{(2\pi)^4} \frac{c_1^c}{(q'^2 + s)^4} = \frac{1}{16\pi^2} \int_0^1 dx \int_0^x dy \int_0^y dz \frac{c_1^c}{s^2} ,$$

$$c_1^c = 2(-2+x-y)(-2+2x-2y+z) , \quad (75)$$

$$d_1 = -i6 \int_0^1 dx \int_0^x dy \int_0^y dz \frac{d^4 q'}{(2\pi)^4} \frac{d_1^b \vec{q}'^2 + d_1^c}{(q'^2 + s)^4} = \frac{1}{32\pi^2} \int_0^1 dx \int_0^x dy \int_0^y dz \left(\frac{-3d_1^b}{s} + \frac{2d_1^c}{s^2} \right) ,$$

$$d_1^b = \frac{5}{3}(-2+x-y) ,$$

$$d_1^c = (-2+x-y)(-2(-1+x-y)(1+z)\vec{k} \cdot \vec{p}_1 + (x^2 - 2x(1+y) + y(2+y))\vec{p}_1^2) , \quad (76)$$

and

$$s_1 = (p_1^2 + M_1^2 - m_3^2)x + (P^2 - M_2^2 - p_1^2 + m_3^2)y + (-2Pk - M_3^2 + M_2^2)z - M_1^2 - (p_1x + (P - p_1)y - kz)^2 . \quad (77)$$

Where we have taken the trace in the terms proportional to $q'_l q'_m$. Also, we have used the formulas $\int \frac{d^4 q}{(q^2+s)^4} = \frac{i\pi^2}{6s^2}$, $\int \frac{d^4 q q^2}{(q^2+s)^4} = \frac{i\pi^2}{3s}$ and $\int \frac{d^4 q \vec{q}^2}{(q^2+s)^4} = -\frac{i\pi^2}{4s}$.

The coefficients in Eq. (54),

$$a_2 = -i6 \int_0^1 dx \int_0^x dy \int_0^y dz \frac{d^4 q'}{(2\pi)^4} \frac{q'^2}{(q'^2 + s_2)^4} = \frac{1}{8\pi^2} \int_0^1 dx \int_0^x dy \int_0^y dz \frac{1}{s_2} , \quad (78)$$

$$c = -i6 \int_0^1 dx \int_0^x dy \int_0^y dz \frac{d^4 q'}{(2\pi)^4} \frac{C^c}{(q'^2 + s_2)^4} = \frac{1}{16\pi^2} \int_0^1 dx \int_0^x dy \int_0^y dz \frac{c^c}{s_2^2} ,$$

$$c_2^c = -4(2+x^2+y^2+y(3-2z)-3z+z^2+x(-3-2y+2z)) , \quad (79)$$

$$d_2 = 0 ,$$

and

$$s_2 = (-M_2^2 + m_3^2 + P^2 - p_1^2)y + (M_2^2 - m_4^2 - P^2 + 2kp_1 + p_1^2)z + (M_1^2 - m_3^2 + p_1^2)x - (p_1x + (P - p_1)y + (k - P + p_1)z)^2 - M_1^2 . \quad (80)$$

The coefficient a_3 in Eq. (57),

$$a_3 = -i2 \int_0^1 dx \int_0^x dy \frac{d^4 q'}{(2\pi)^4} \frac{(2-y)}{(q'^2 + s_3)^3} = \frac{1}{16\pi^2} \int_0^1 dx \int_0^x dy \frac{(2-y)}{s} \quad (81)$$

$$s_3 = -M_1^2 + (M_1^2 - M_2^2 + P^2)x + (k^2 + M_2^2 - m_3^2 - P^2 + 2kp_1 + p_1^2)y - (Px + (k - P + p_1)y)^2 , \quad (82)$$

A.4 Decay of $R_c(S_c)$ to $DD_{(s)}^*$: Coefficients C_V and C_P in Eqs. (39) and (40).

Coefficients needed in Eqs. (39) and (40), C_V and C_P , for the evaluation of the decay $R_{cc} \rightarrow DD_{(s)}^*$.

V_1	V_2	m_l	m	V	I	A	P_V	C_P
D^{*+}	D^{*0}	π^0	D^+	D^{*0}	$-\frac{1}{\sqrt{2}}$	$-\frac{1}{2}$	$\frac{1}{\sqrt{2}}$	$\frac{1}{4}$
D^{*+}	D^{*0}	η	D^+	D^{*0}	$-\frac{1}{\sqrt{2}}$	$-\frac{1}{\sqrt{6}}$	$-\frac{1}{\sqrt{3}}$	$-\frac{1}{6}$
D^{*+}	D^{*0}	η'	D^+	D^{*0}	$-\frac{1}{\sqrt{2}}$	$-\frac{1}{2\sqrt{3}}$	$-\frac{1}{\sqrt{6}}$	$-\frac{1}{12}$
D^{*+}	D^{*0}	η_c	D^+	D^{*0}	$-\frac{1}{\sqrt{2}}$	$-\frac{1}{\sqrt{2}}$	1	$\frac{1}{2}$
D^{*0}	D^{*+}	π^-	D^+	D^{*0}	$\frac{1}{\sqrt{2}}$	$-\frac{1}{\sqrt{2}}$	-1	$\frac{1}{2}$
D^{*0}	D^{*+}	π^0	D^0	D^{*+}	$\frac{1}{\sqrt{2}}$	$\frac{1}{2}$	$-\frac{1}{\sqrt{2}}$	$-\frac{1}{4}$
D^{*0}	D^{*+}	η	D^0	D^{*+}	$\frac{1}{\sqrt{2}}$	$-\frac{1}{\sqrt{6}}$	$-\frac{1}{\sqrt{3}}$	$\frac{1}{6}$
D^{*0}	D^{*+}	η'	D^0	D^{*+}	$\frac{1}{\sqrt{2}}$	$-\frac{1}{2\sqrt{3}}$	$-\frac{1}{\sqrt{6}}$	$\frac{1}{12}$
D^{*0}	D^{*+}	η_c	D^0	D^{*+}	$\frac{1}{\sqrt{2}}$	$-\frac{1}{\sqrt{2}}$	1	$-\frac{1}{2}$
D^{*+}	D^{*0}	π^+	D^0	D^{*+}	$-\frac{1}{\sqrt{2}}$	$-\frac{1}{\sqrt{2}}$	-1	$-\frac{1}{2}$

Table 6: Coefficient C_P in Eq. (39) for R_{cc}^+ .

V_1	V_2	V_l	m	V	I	A	P_V	C_V
D^{*+}	D^{*0}	ρ^0	D^+	D^{*0}	$-\frac{1}{\sqrt{2}}$	$-\frac{1}{2}$	$\frac{1}{\sqrt{2}}$	$\frac{1}{4}$
D^{*+}	D^{*0}	ω	D^+	D^{*0}	$-\frac{1}{\sqrt{2}}$	$\frac{1}{2}$	$\frac{1}{\sqrt{2}}$	$-\frac{1}{4}$
D^{*+}	D^{*0}	J/ψ	D^+	D^{*0}	$-\frac{1}{\sqrt{2}}$	$\frac{1}{\sqrt{2}}$	-1	$\frac{1}{2}$
D^{*0}	D^{*+}	ρ^+	D^+	D^{*0}	$\frac{1}{\sqrt{2}}$	$\frac{1}{\sqrt{2}}$	1	$\frac{1}{2}$
D^{*0}	D^{*+}	ρ^0	D^0	D^{*+}	$\frac{1}{\sqrt{2}}$	$\frac{1}{2}$	$-\frac{1}{\sqrt{2}}$	$-\frac{1}{4}$
D^{*0}	D^{*+}	ω	D^0	D^{*+}	$\frac{1}{\sqrt{2}}$	$\frac{1}{2}$	$\frac{1}{\sqrt{2}}$	$\frac{1}{4}$
D^{*0}	D^{*+}	J/ψ	D^0	D^{*+}	$\frac{1}{\sqrt{2}}$	$\frac{1}{\sqrt{2}}$	-1	$-\frac{1}{2}$
D^{*+}	D^{*0}	ρ^-	D^0	D^{*+}	$-\frac{1}{\sqrt{2}}$	$\frac{1}{\sqrt{2}}$	1	$-\frac{1}{2}$

Table 7: Coefficient C_V in Eq. (39) for R_{cc}^+ .

V_1	V_2	m_l	m	V	I	A	P_V	C_P
D_s^{*+}	D^{*0}	η	D_s^+	D^{*0}	-1	$-\frac{1}{\sqrt{6}}$	$\frac{1}{\sqrt{3}}$	$\frac{1}{3\sqrt{2}}$
D_s^{*+}	D^{*0}	η'	D_s^+	D^{*0}	-1	$-\frac{1}{2\sqrt{3}}$	$-\sqrt{\frac{2}{3}}$	$-\frac{1}{3\sqrt{2}}$
D_s^{*+}	D^{*0}	η_c	D_s^+	D^{*0}	-1	$-\frac{1}{\sqrt{2}}$	1	$\frac{1}{\sqrt{2}}$
D^{*0}	D_s^{*+}	K^-	D_s^+	D^{*0}	-1	$-\frac{1}{\sqrt{2}}$	-1	$-\frac{1}{\sqrt{2}}$
D^{*0}	D_s^{*+}	η	D^0	D_s^{*+}	-1	$\frac{1}{\sqrt{6}}$	$-\frac{1}{\sqrt{3}}$	$\frac{1}{3\sqrt{2}}$
D^{*0}	D_s^{*+}	η'	D^0	D_s^{*+}	-1	$-\frac{1}{\sqrt{3}}$	$-\frac{1}{\sqrt{6}}$	$-\frac{1}{3\sqrt{2}}$
D^{*0}	D_s^{*+}	η_c	D^0	D_s^{*+}	-1	$-\frac{1}{\sqrt{2}}$	1	$\frac{1}{\sqrt{2}}$
D_s^{*+}	D^{*0}	K^+	D^0	D_s^{*+}	-1	$-\frac{1}{\sqrt{2}}$	-1	$-\frac{1}{\sqrt{2}}$

Table 8: Coefficient C_P in Eq. (39) for S_{cc}^+ .

V_1	V_2	V_l	m	V	I	A	P_V	C_V
D_s^{*+}	D^{*0}	J/ψ	D_s^+	D^{*0}	-1	$\frac{1}{\sqrt{2}}$	-1	$\frac{1}{\sqrt{2}}$
D^{*0}	D_s^{*+}	K^{*+}	D_s^+	D^{*0}	-1	$\frac{1}{\sqrt{2}}$	1	$-\frac{1}{\sqrt{2}}$
D^{*0}	D_s^{*+}	J/ψ	D^0	D_s^{*+}	-1	$\frac{1}{\sqrt{2}}$	-1	$\frac{1}{\sqrt{2}}$
D^{*0}	D_s^{*+}	K^{*-}	D^0	D_s^{*+}	-1	$\frac{1}{\sqrt{2}}$	-1	$\frac{1}{\sqrt{2}}$

Table 9: Coefficients C_V in Eq. (39) for S_{cc}^+ .

V_1	V_2	m_l	m	V	I	A	P_V	C_P
D_s^{*+}	D^{*+}	η	D_s^+	D^{*+}	1	$-\frac{1}{\sqrt{6}}$	$\frac{1}{\sqrt{3}}$	$-\frac{1}{3\sqrt{2}}$
D_s^{*+}	D^{*+}	η'	D_s^+	D^{*+}	1	$-\frac{1}{2\sqrt{3}}$	$-\sqrt{\frac{2}{3}}$	$\frac{1}{3\sqrt{2}}$
D_s^{*+}	D^{*+}	η_c	D_s^+	D^{*+}	1	$-\frac{1}{\sqrt{2}}$	1	$-\frac{1}{\sqrt{2}}$
D^{*+}	D_s^{*+}	\bar{K}^0	D_s^+	D^{*+}	1	$-\frac{1}{\sqrt{2}}$	-1	$\frac{1}{\sqrt{2}}$
D^{*+}	D_s^{*+}	η	D^+	D_s^{*+}	1	$\frac{1}{\sqrt{6}}$	$-\frac{1}{\sqrt{3}}$	$-\frac{1}{3\sqrt{2}}$
D^{*+}	D_s^{*+}	η'	D^+	D_s^{*+}	1	$-\frac{1}{\sqrt{3}}$	$-\frac{1}{\sqrt{6}}$	$\frac{1}{3\sqrt{2}}$
D^{*+}	D_s^{*+}	η_c	D^+	D_s^{*+}	1	$-\frac{1}{\sqrt{2}}$	1	$-\frac{1}{\sqrt{2}}$
D_s^{*+}	D^{*+}	K^0	D^+	D_s^{*+}	1	$-\frac{1}{\sqrt{2}}$	-1	$\frac{1}{\sqrt{2}}$

Table 10: Coefficient C_P in Eq. (39) for S_{cc}^{++} .

V_1	V_2	V_l	m	V	I	A	P_V	C_V
D_s^{*+}	D^{*+}	J/ψ	D_s^+	D^{*+}	1	$\frac{1}{\sqrt{2}}$	-1	$-\frac{1}{\sqrt{2}}$
D^{*+}	D_s^{*+}	\bar{K}^{*0}	D_s^+	D^{*+}	1	$\frac{1}{\sqrt{2}}$	1	$\frac{1}{\sqrt{2}}$
D^{*+}	D_s^{*+}	J/ψ	D^+	D_s^{*+}	1	$\frac{1}{\sqrt{2}}$	-1	$-\frac{1}{\sqrt{2}}$
D_s^{*+}	D^{*+}	K^{*0}	D^+	D_s^{*+}	1	$\frac{1}{\sqrt{2}}$	1	$\frac{1}{\sqrt{2}}$

Table 11: Coefficient C_V in Eq. (39) for S_{cc}^{++} .

A.5 Direct decay of $R_c(S_c)$ to $DD\gamma$: Coefficients \mathcal{A} , \mathcal{B} and \mathcal{C} in Eqs. (58), (60) and (61).

Coefficients needed for the evaluation of the diagrams depicted in Fig. 6) 1) – 3), \mathcal{A} , \mathcal{B} and \mathcal{C} in Eqs. (58), (60) and (61).

V_1	V_2	V_3	m_3	m_1	m_2	V_l	\mathcal{P}	P_{V_1}	P_{V_2}	V_3	I	\mathcal{A}
D^{*0}	D^{*+}	D^{*+}	π^0	D^0	D^+	ρ^0	$\frac{1}{\sqrt{2}}$	$-\frac{1}{\sqrt{2}}$	$-\frac{1}{\sqrt{2}}$	$\frac{1}{\sqrt{2}}$	$\pm\frac{1}{\sqrt{2}}$	$\frac{1}{4\sqrt{2}}$
			η				$-\frac{1}{\sqrt{3}}$	$\frac{1}{\sqrt{3}}$			$-\frac{1}{6\sqrt{2}}$	
			η'				$-\frac{1}{\sqrt{6}}$	$\frac{1}{\sqrt{6}}$			$-\frac{1}{12\sqrt{2}}$	
			η_c				1	-1			$-\frac{1}{2\sqrt{2}}$	
D^{*0}	D^{*+}	D^{*+}	π^0	D^+	D^0	ω	$\frac{1}{3\sqrt{2}}$	$-\frac{1}{\sqrt{2}}$	$-\frac{1}{\sqrt{2}}$	$-\frac{1}{\sqrt{2}}$	$\pm\frac{1}{\sqrt{2}}$	$-\frac{1}{12\sqrt{2}}$
			η				$-\frac{1}{\sqrt{3}}$	$\frac{1}{\sqrt{3}}$			$\frac{1}{18\sqrt{2}}$	
			η'				$-\frac{1}{\sqrt{6}}$	$\frac{1}{\sqrt{6}}$			$\frac{1}{36\sqrt{2}}$	
			η_c				1	-1			$\frac{1}{6\sqrt{2}}$	
D^{*0}	D^{*+}	D^{*+}	π^0	D^+	D^0	J/ψ	$\frac{2}{3}$	$-\frac{1}{\sqrt{2}}$	$-\frac{1}{\sqrt{2}}$	1	$\pm\frac{1}{\sqrt{2}}$	$\frac{1}{3\sqrt{2}}$
			η				$-\frac{1}{\sqrt{3}}$	$\frac{1}{\sqrt{3}}$			$-\frac{\sqrt{2}}{9}$	
			η'				$-\frac{1}{\sqrt{6}}$	$\frac{1}{\sqrt{6}}$			$-\frac{1}{9\sqrt{2}}$	
			η_c				1	-1			$-\frac{\sqrt{2}}{3}$	
D^{*0}	D^{*+}	D^{*+}	π^-	D^+	D^0	ρ^0	$\frac{1}{\sqrt{2}}$	-1	1	$\frac{1}{\sqrt{2}}$		$-\frac{1}{2\sqrt{2}}$
						ω	$\frac{1}{3\sqrt{2}}$			$-\frac{1}{\sqrt{2}}$		$\frac{1}{6\sqrt{2}}$
						J/ψ	$\frac{2}{3}$			1		$-\frac{\sqrt{2}}{3}$

Table 12: Coefficient \mathcal{A} in Eqs. (58), (60) and (61) for R_{cc}^+ .

V_1	V_2	V_3	m_3	m_1	m_2	V_l	\mathcal{P}	P_{V_1}	P_{V_2}	V_3	I	\mathcal{A}
D^{*0}	D_s^{*+}	D_s^{*+}	K^-	D_s^+	D^0	ϕ	$-\frac{1}{3}$	-1	1	-1	-1	$\frac{1}{3}$
						J/ψ	$\frac{2}{3}$			1		$\frac{2}{3}$
D^{*0}	D_s^{*+}	D_s^{*+}	η	D^0	D_s^+	ϕ	$-\frac{1}{3}$	$-\frac{1}{\sqrt{3}}$	$-\frac{1}{\sqrt{3}}$	-1	-1	$-\frac{1}{9}$
			η'					$-\frac{1}{\sqrt{6}}$	$\sqrt{\frac{2}{3}}$			$\frac{1}{9}$
			η_c					1	-1			$\frac{1}{3}$
			η			J/ψ	$\frac{2}{3}$	$-\frac{1}{\sqrt{3}}$	$-\frac{1}{\sqrt{3}}$	1	-1	$-\frac{2}{9}$
			η'					$-\frac{1}{\sqrt{6}}$	$\sqrt{\frac{2}{3}}$			$\frac{2}{9}$
			η_c					1	-1			$\frac{2}{3}$

Table 13: Coefficient \mathcal{A} in Eqs. (58), (60) and (61) for S_{cc}^+ .

V_1	V_2	V_3	m_3	m_1	m_2	V_l	\mathcal{P}	P_{V_1}	P_{V_2}	V_3	I	\mathcal{A}
D^{*+}	D_s^{*+}	D_s^{*+}	\bar{K}^0	D_s^+	D^+	ϕ	$-\frac{1}{3}$	-1	1	-1	1	$-\frac{1}{3}$
						J/ψ	$\frac{2}{3}$	-1	1	1	1	$-\frac{2}{3}$
D^{*+}	D_s^{*+}	D_s^{*+}	η	D^+	D_s^+	ϕ	$-\frac{1}{3}$	$-\frac{1}{\sqrt{3}}$	$-\frac{1}{\sqrt{3}}$	-1	1	$\frac{1}{9}$
			η'					$-\frac{1}{\sqrt{6}}$	$\sqrt{\frac{2}{3}}$			$-\frac{1}{9}$
			η_c					1	-1			$-\frac{1}{3}$
D^{*+}	D_s^{*+}	D_s^{*+}	η	D^+	D_s^+	J/ψ	$\frac{2}{3}$	$-\frac{1}{\sqrt{3}}$	$-\frac{1}{\sqrt{3}}$	1	1	$\frac{2}{9}$
			η'					$-\frac{1}{\sqrt{6}}$	$\sqrt{\frac{2}{3}}$			$-\frac{2}{9}$
			η_c					1	-1			$-\frac{2}{3}$
D_s^{*+}	D^{*+}	D^{*+}	\bar{K}^0	D^+	D_s^+	ρ^0	$\frac{1}{\sqrt{2}}$	-1	1	$\frac{1}{\sqrt{2}}$	1	$-\frac{1}{2}$
						ω	$\frac{1}{3\sqrt{2}}$	-1	1	$-\frac{1}{\sqrt{2}}$	1	$\frac{1}{6}$
						J/ψ	$\frac{2}{3}$	-1	1	1	1	$-\frac{2}{3}$
D_s^{*+}	D^{*+}	D^{*+}	η	D_s^+	D^+	ρ	$\frac{1}{\sqrt{2}}$	$\frac{1}{\sqrt{3}}$	$\frac{1}{\sqrt{3}}$	$\frac{1}{\sqrt{2}}$	1	$\frac{1}{6}$
			η'					$-\sqrt{\frac{2}{3}}$	$\frac{1}{\sqrt{6}}$			$-\frac{1}{6}$
			η_c					1	-1			$-\frac{1}{2}$
D_s^{*+}	D^{*+}	D^{*+}	η	D_s^+	D^+	ω	$\frac{1}{3\sqrt{2}}$	$\frac{1}{\sqrt{3}}$	$\frac{1}{\sqrt{3}}$	$-\frac{1}{\sqrt{2}}$	1	$-\frac{1}{18}$
			η'					$-\sqrt{\frac{2}{3}}$	$\frac{1}{\sqrt{6}}$			$\frac{1}{18}$
			η_c					1	-1			$\frac{1}{6}$
D_s^{*+}	D^{*+}	D^{*+}	η	D_s^+	D^+	J/ψ	$\frac{2}{3}$	$\frac{1}{\sqrt{3}}$	$\frac{1}{\sqrt{3}}$	1	1	$\frac{2}{9}$
			η'					$-\sqrt{\frac{2}{3}}$	$\frac{1}{\sqrt{6}}$			$-\frac{2}{9}$
			η_c					1	-1			$-\frac{2}{3}$

Table 14: Coefficient \mathcal{A} in Eqs. (58), (60) and (61) for S_{cc}^{++} .

V_1	V_2	m_3	m_4	m_1	m_2	V_l	\mathcal{P}	P_{V_1}	P_{V_2}	P_{V_3}	\mathcal{B}
D^{*+}	D^{*0}	π^+	π^-	D^0	D^+	ρ^0	$\frac{1}{\sqrt{2}}$	-1	1	$\sqrt{2}$	$\frac{1}{\sqrt{2}}$
D_s^{*+}	D^{*0}	K^+	K^-	D^0	D_s^+	ρ^0	$\frac{1}{\sqrt{2}}$	-1	1	$\frac{1}{\sqrt{2}}$	$\frac{1}{2}$
						ω	$\frac{1}{3\sqrt{2}}$			$\frac{1}{\sqrt{2}}$	$\frac{1}{6}$
						ϕ	$-\frac{1}{3}$			-1	$\frac{1}{3}$

Table 15: Coefficient \mathcal{B} in Eqs. (58), (60) and (61).

V_1	V_2	m_3	m_1	m_2	$V_{2P\gamma}$	P_{V_1}	I	\mathcal{C}
D^{*0}	D^{*+}	π^+	D^+	D^0	-2	1	$\pm\frac{1}{\sqrt{2}}$	$-\sqrt{2}$
D^{*+}	D^{*0}	π^-	D^0	D^+	1	1		$-\frac{1}{\sqrt{2}}$
D^{*+}	D^{*0}	π^0	D^+	D^0	$\frac{1}{\sqrt{2}}$	$\frac{1}{\sqrt{2}}$		$-\frac{1}{2\sqrt{2}}$
		η			$-\frac{1}{\sqrt{3}}$	$\frac{1}{\sqrt{3}}$		$\frac{1}{3\sqrt{2}}$
		η'			$-\frac{1}{\sqrt{6}}$	$\frac{1}{\sqrt{6}}$		$\frac{1}{6\sqrt{2}}$
		η_c			1	-1		$\frac{1}{\sqrt{2}}$
D^{*0}	D_s^{*+}	K^+	D_s^+	D^0	-2	1	-1	2
D_s^{*+}	D^{*0}	K^-	D^0	D_s^+	1	1	-1	-1
D_s^{*+}	D^{*0}	η	D_s^+	D^0	$\frac{1}{\sqrt{3}}$	$\frac{1}{\sqrt{3}}$		$-\frac{1}{3}$
		η'			$-\sqrt{\frac{2}{3}}$	$\frac{1}{\sqrt{6}}$		$\frac{1}{3}$
		η_c			1	-1		1

Table 16: Coefficient \mathcal{C} in Eqs. (58), (60) and (61).

V_1	V_2	m_3	m_1	m_2	$V_{2P\gamma}$	P_{V_1}	I	\mathcal{C}
D^{*0}	D^{*+}	π^+	D^+	D^0	-2	1	$\pm\frac{1}{\sqrt{2}}$	$-\sqrt{2}$
D^{*+}	D^{*0}	π^-	D^0	D^+	1	1		$-\frac{1}{\sqrt{2}}$
D^{*+}	D^{*0}	π^0	D^+	D^0	$\frac{1}{\sqrt{2}}$	$\frac{1}{\sqrt{2}}$		$-\frac{1}{2\sqrt{2}}$
		η			$-\frac{1}{\sqrt{3}}$	$\frac{1}{\sqrt{3}}$		$\frac{1}{3\sqrt{2}}$
		η'			$-\frac{1}{\sqrt{6}}$	$\frac{1}{\sqrt{6}}$		$\frac{1}{6\sqrt{2}}$
		η_c			1	-1		$\frac{1}{\sqrt{2}}$
D^{*0}	D_s^{*+}	K^+	D_s^+	D^0	-2	1	-1	2
D_s^{*+}	D^{*0}	K^-	D^0	D_s^+	1	1	-1	-1
D_s^{*+}	D^{*0}	η	D_s^+	D^0	$\frac{1}{\sqrt{3}}$	$\frac{1}{\sqrt{3}}$	-1	$-\frac{1}{3}$
		η'			$-\sqrt{\frac{2}{3}}$	$\frac{1}{\sqrt{6}}$		$\frac{1}{3}$
		η_c			1	-1		1
D_s^{*+}	D^{*+}	η	D_s^+	D^+	$\frac{1}{\sqrt{3}}$	$\frac{1}{\sqrt{3}}$	1	$\frac{1}{3}$
D_s^{*+}	D^{*+}	η'	D_s^+	D^+	$-\sqrt{\frac{2}{3}}$	$\frac{1}{\sqrt{6}}$	1	$-\frac{1}{3}$
D_s^{*+}	D^{*+}	η_c	D_s^+	D^+	1	-1	1	-1
D_s^{*+}	D^{*+}	\bar{K}^0	D^+	D_s^+	-1	1	1	-1
D^{*+}	D_s^{*+}	η	D^+	D_s^+	$-\frac{1}{\sqrt{3}}$	$-\frac{1}{\sqrt{3}}$	1	$\frac{1}{3}$
		η'			$-\frac{1}{\sqrt{6}}$	$\sqrt{\frac{2}{3}}$	1	$-\frac{1}{3}$
		η_c			1	-1	1	-1
D^{*+}	D_s^{*+}	K^0	D_s^+	D^+	-1	1	1	-1

Table 17: Coefficient \mathcal{C} in Eqs. (58), (60) and (61).

References

- [1] S. K. Choi *et al.* [Belle Collaboration], Phys. Rev. Lett. **91**, 262001 (2003)
- [2] S. Godfrey and S. L. Olsen, Ann. Rev. Nucl. Part. Sci. **58**, 51 (2008)
- [3] F. E. Close and P. R. Page, Phys. Lett. B **578**, 119 (2004). C. -Y. Wong, Phys. Rev. C **69**, 055202 (2004). S. Pakvasa and M. Suzuki, Phys. Lett. B **579**, 67 (2004). M. B. Voloshin, Phys. Lett. B **604**, 69 (2004).
E. S. Swanson, Phys. Lett. B **588**, 189 (2004).
E. Braaten and M. Kusunoki, Phys. Rev. D **72**, 054022 (2005).

- M. B. Voloshin and L. B. Okun, JETP Lett. **23**, 333 (1976) [Pisma Zh. Eksp. Teor. Fiz. **23**, 369 (1976)].
- A. De Rujula, H. Georgi and S. L. Glashow, Phys. Rev. Lett. **38**, 317 (1977).
- N. A. Tornqvist, hep-ph/0308277. M. B. Voloshin, Phys. Lett. B **579**, 316 (2004).
- [4] N. A. Tornqvist, Z. Phys. C **61**, 525 (1994).
- [5] D. Gamermann and E. Oset, Phys. Rev. D **80**, 014003 (2009). D. Gamermann and E. Oset, Eur. Phys. J. A **33**, 119 (2007).
- [6] D. Gamermann, J. Nieves, E. Oset and E. Ruiz Arriola, Phys. Rev. D **81**, 014029 (2010)
- [7] M. Bando, T. Kugo, S. Uehara, K. Yamawaki and T. Yanagida, Phys. Rev. Lett. **54**, 1215 (1985). M. Bando, T. Kugo and K. Yamawaki, Phys. Rept. **164**, 217 (1988). M. Harada and K. Yamawaki, Phys. Rept. **381**, 1 (2003). U. G. Meißner, Phys. Rept. **161**, 213 (1988).
- [8] H. Nagahiro, L. Roca, A. Hosaka and E. Oset, Phys. Rev. D **79** (2009) 014015
- [9] M. Takizawa and S. Takeuchi, arXiv:1206.4877 [hep-ph].
- [10] R. Aaij et al. (LHCb Collaboration) , Phys. Rev. Lett. **110**, 222001 (2013).
- [11] R. Molina and E. Oset, Phys. Rev. D **80**, 114013 (2009)
- [12] T. Branz, T. Gutsche and V. E. Lyubovitskij, Phys. Rev. D **80**, 054019 (2009)
- [13] J. Nieves and M. P. Valderrama, Phys. Rev. D **86**, 056004 (2012)
- [14] F.-K. Guo, J. Haidenbauer, C. Hanhart and U.-G. Meißner, Phys. Rev. D **82**, 094008 (2010).
- [15] X. Liu, Z. G. Luo, Y. R. Liu and S. L. Zhu, Eur. Phys. J. C **61**, 411 (2009)
- [16] G. -J. Ding, W. Huang, J. -F. Liu and M. -L. Yan, Phys. Rev. D **79**, 034026 (2009)
- [17] G. -J. Ding, Phys. Rev. D **79**, 014001 (2009)
- [18] A. Martinez Torres, K. P. Khemchandani, D. Gamermann and E. Oset, Phys. Rev. D **80**, 094012 (2009)
- [19] P. G. Ortega, J. Segovia, D. R. Entem and F. Fernandez, Phys. Rev. D **81**, 054023 (2010)
- [20] Q. Wang, C. Hanhart and Q. Zhao, Phys. Rev. Lett. **111**, 132003 (2013)
- [21] C. W. Xiao, J. Nieves and E. Oset, Phys. Rev. D **88**, 056012 (2013)

- [22] R. Molina, H. Nagahiro, A. Hosaka and E. Oset, Phys. Rev. D **80**, 014025 (2009)
- [23] R. Molina, T. Branz and E. Oset, Phys. Rev. D **82**, 014010 (2010)
- [24] T. F. Carames, A. Valcarce and J. Vijande, Phys. Lett. B **699**, 291 (2011). J. Vijande, A. Valcarce and J. -M. Richard, Phys. Rev. D **76**, 114013 (2007)
- [25] Y. Cui, X. -L. Chen, W. -Z. Deng and S. -L. Zhu, High Energy Phys. Nucl. Phys. **31**, 7 (2007)
- [26] F. S. Navarra, M. Nielsen and S. H. Lee, Phys. Lett. B **649**, 166 (2007)
- [27] T. Hyodo, Y. -R. Liu, M. Oka, K. Sudoh and S. Yasui, Phys. Lett. B **721**, 56 (2013)
- [28] R. Molina, D. Nicmorus and E. Oset, Phys. Rev. D **78**, 114018 (2008)
- [29] L. S. Geng and E. Oset, Phys. Rev. D **79**, 074009 (2009)
- [30] Riazuddin and Fayyazuddin, Phys. Rev. **147**, 1071 (1966)
- [31] J.J. Sakurai, Currents and mesons (University of Chicago Press, Chicago Il 1969)
- [32] J. Beringer *et al.* [Particle Data Group], Phys. Rev. D **86**, 010001 (2012)
- [33] J. A. Oller and E. Oset, Nucl. Phys. A **620**, 438 (1997) [Erratum-ibid. A **652**, 407 (1999)]
- [34] S. Weinberg, Phys. Rev. **130**, 776 (1963). S. Weinberg, Phys. Rev. **131**, 440 (1963). S. Weinberg, Phys. Rev. **137**, B672 (1965).
- [35] F. -K. Guo, C. Hanhart and U. -G. Meissner, Phys. Rev. Lett. **102**, 242004 (2009)
- [36] D. Gamermann, E. Oset and B. S. Zou, Eur. Phys. J. A **41**, 85 (2009)
- [37] F. Aceti, R. Molina and E. Oset, Phys. Rev. D **86**, 113007 (2012)
- [38] R. Molina, H. Nagahiro, A. Hosaka and E. Oset, Phys. Rev. D **83**, 094030 (2011)
- [39] A. Ocherashvili *et al.* [SELEX Collaboration], Phys. Lett. B **628**, 18 (2005)
- [40] B. Aubert *et al.* [BaBar Collaboration], Phys. Rev. D **74**, 011103 (2006)
- [41] R. Chistov *et al.* [BELLE Collaboration], Phys. Rev. Lett. **97**, 162001 (2006)
- [42] P. Pakhlov *et al.* [Belle Collaboration], Phys. Rev. D **79**, 071101 (2009)